Estimated Future Mortality from Pathogens of Epidemic and Pandemic Potential

Nita K. Madhav, Ben Oppenheim, Nicole Stephenson, Rinette Badker,
Dean T. Jamison, Cathine Lam, and Amanda Meadows

Abstract

Epidemics and pandemics pose a sporadic and sometimes severe threat to human health. How should policymakers prioritize preventing and preparing for such events, relative to other needs? To answer this question, we used computational epidemiology and extreme events modeling simulations to estimate the risk of future mortality from low frequency, high severity epidemics and pandemics in two important categories—respiratory diseases (in particular those caused by pandemic influenza viruses and novel coronaviruses) and viral hemorrhagic fevers (VHFs) such as Ebola and Marburg virus diseases. We estimate a global annual average of 2.5 million deaths, attributed to respiratory pandemics. We estimate an annual average of 26,000 VHF deaths globally, 72 percent of which would be in Africa. Annual averages conceal vast year by year variation, and the reported analyses convey that variation—as well as variation across regions and by age. Our estimates suggest that both the frequency and severity of such events is higher than previously believed—and this is likely to be a lower bound estimate given the focus of this chapter on deaths caused by a subset of pathogens. Our simulations suggest that an event having the mortality level of COVID-19 should not be considered a "once in a century" risk, but rather occurring with an annual probability of 2–3 percent (that is, a one in 33–50-year event). Despite the substantial uncertainty in heavy-tail distributions, policymakers can use these estimates to develop risk-informed financing, prevention, preparedness, and response plans.

KEYWORDS

Epidemics, pandemics, influenza, coronavirus, risk modeling

Estimated Future Mortality from Pathogens of Epidemic and Pandemic Potential

Nita K. Madhav
Ginkgo Bioworks
nmadhav@ginkgobioworks.com

Ben Oppenheim
Ginkgo Bioworks

Nicole Stephenson
Ginkgo Bioworks

Rinette Badker
Ginkgo Bioworks

Dean T. Jamison
University of California, San Francisco

Cathine Lam
Ginkgo Bioworks

Amanda Meadows
Ginkgo Bioworks

Certain supporting data and code are publicly available in the following repositories:

- Zoonotic disease data—https://github.com/concentricbyginkgo/zoonotic_spillover_trend
- Underreporting—https://github.com/metabiota-ameadows/underreporting
- COVID-19 dataset—https://data.humdata.org/dataset/2019-novel-coronavirus-cases

Other data and model code are considered commercial/proprietary and cannot be publicly released.

Contents

List of Figures

List of Tables

Foreword

The Center for Global Development (CGD) is publishing this working paper because the paper's estimates of the risk of the next pandemic were essential for informing recent work including a Resource Allocation Framework for Pandemic Risk and Surveillance, prepared in collaboration with Concentric by Ginkgo Bioworks, which in turn sought to contribute to policy discussions about the design and implementation of the Pandemic Fund. The Pandemic Fund went into implementation based on a proposal from the G20 High-Level Independent Panel Report on Financing the Global Commons for Pandemic Preparedness and Response, co-chaired by Ngozi Okonjo-Iweala, Lawrence Summers (CGD board chair), and Tharman Shanmugaratnam, with CGD and Bruegel as the project team and the US National Academy of Medicine and Wellcome Trust as administrative secretariat.

This paper will be invaluable in informing policy discussions about the future of pandemic financing amidst competing policy agendas. It offers estimates of pandemic risk, and emphasizes the importance of "tail risk," indicating the potential impact of highly severe yet rare events. Compared to a paper by Fan, Jamison, and Summers (2017) on pandemic losses, the estimates from this paper are much larger.

This working paper was prepared as one of many chapters in the fourth edition of the Disease Control Priorities (DCP), hosted by the Bergen Centre for Ethics and Priority Setting at University of Bergen under the directorship of Ole Norheim and to be published by the World Bank. The first edition of the DCP was published as part of the World Development Report (WDR) in 1993. That report, entitled "Investing in Health," was the World Bank's first-ever WDR on health. It was led by Lawrence Summers (then chief economist at the World Bank) and Dean Jamison, who led subsequent editions of DCP nearly every decade. Priority setting for health, informed by economic evidence and value for money, remains as important as ever before in this era of polycrises, to help ensure that every cent spent on health care improves and saves lives.

Victoria Fan
Senior Fellow
Center for Global Development

Introduction

Long before the emergence of COVID-19, policy analysts described pandemics as a "neglected dimension" of global security, because fundamental aspects of prevention and preparedness were (and continue to be) persistently underfinanced (Jamison et al., 2013, Sands et al., 2016). Several high-level panels convened in the midst of the COVID-19 pandemic have called for large increases in global spending on health system strengthening, surveillance, and preparedness (Sirleaf & Clark, 2021). These recommendations are vital, but contend with an entrenched pattern of panic and neglect—a strong tendency for sporadic health emergencies to spark short-term attention and investment, which tails off all too rapidly once the crisis has passed.

The slide from panic to neglect happens in part because policymakers are operating under uncertainty; they lack estimates of the probability of epidemics—including pandemics (Table 1)—that would enable them to prioritize preparedness for such events relative to other needs. As a result, epidemics and pandemics tend to be treated as inevitable and unpredictable phenomena rather than events for which decision makers can perform rigorous analysis, estimate costs, and prioritize investments. A key objective of this chapter is to reduce some dimensions of uncertainty in the analysis of epidemics and pandemics by applying principles of risk management: a framework in which probabilities can be estimated sufficiently to guide decision-making.

Policymakers often choose to prioritize preparedness for high-probability events rather than rare ones, as the benefits of preparing for infrequent events are often invisible (Lempert & Light, 2009). To grapple with the threat posed by infrequent, severe epidemics, analysts should adopt a risk-based approach for decision-making, more akin to methods used for other natural catastrophes. Emergency planners and policymakers are accustomed to thinking about natural catastrophes, such as floods and earthquakes, in terms of their frequency and severity (FEMA, 2016). This chapter provides a framework for quantifying the risk of epidemics, which can be used to change the dominant paradigm for risk assessment and preparedness planning. This framework is not typically used to plan for epidemics—but could be.

Adopting the most cost-effective strategies to prevent, prepare for, and respond to epidemics requires an understanding of their anticipated frequency and severity—that is, the level of risk that they pose (Table 1). Interventions such as strengthening disease surveillance systems, investing in lab and diagnostic capacity, and developing new vaccine platforms, production systems and supply chains might have a modest benefit-cost ratio if severe pandemics are merely a "once in a century" risk, but—if the risk is substantially greater—might be very cost-effective strategies to protect global health and reduce mortality. Our risk estimates allow decision makers to approximate the necessary level of epidemic preparedness measures, and to identify which measures would be most cost-effective, both during and between epidemic periods.

In this chapter, we estimate the mortality risk of future epidemics caused by key respiratory pathogens and viral hemorrhagic fevers. We present new evidence and analyses of simulations underscoring the substantial risk posed by epidemics. In DCP-3, Madhav et al. (2017) presented risk estimates focusing on pandemic influenza—only one, albeit critical, pathogenic risk. In this chapter, we expand on this foundation and update the risk estimates provided in DCP-3 to include estimates for a broader set of epidemic risks. We incorporated new data and scientific advances into model enhancements, which we developed in part to support multilateral agencies, governments, philanthropic organizations, and the private sector. These enhancements also account for under-reporting in epidemiological data and adjust for demographic changes since Madhav et al. (2017) was originally published.

While many pathogens are capable of sparking large infectious disease events (e.g., pandemic influenza viruses, Zika virus, coronaviruses, HIV, cholera, dengue virus, and more [Madhav et al., 2017]), we focused our analysis for this chapter in part based on Fraser et al.'s (2004) framework for assessing the controllability of epidemics caused by different pathogenic threats. In that framework, risk of an uncontrollable epidemic increases with human-to-human transmission efficiency and decreases with detection probability. Therefore, we focus this chapter on a subset of pathogens that meet these criteria and comprise the majority of risk: respiratory diseases, notably those caused by pandemic influenza viruses and epidemic/novel coronaviruses. We also develop estimates for viral hemorrhagic fevers (VHFs), encompassing filoviruses (e.g., Ebola and Marburg viruses), and Nipah virus (Table 1). These pathogens are of global concern and meet some aspects of Fraser et al.'s criteria, as they have shown the potential for causing asymptomatic infection (Diallo et al., 2019) and evading detection (Glennon et al., 2019).

We regard several other categories of infectious disease threats to be outside the scope of this chapter, and, though we recognize their importance, have not included them in our analysis:

- **endemic diseases**, even if they can enter epidemic phases (e.g., seasonal influenza, HIV/AIDS, and malaria), since these diseases have well-understood, frequently occurring patterns of losses;
- **vector-borne diseases** (e.g., Zika and dengue), since the geographic ranges are constrained by climatic and ecological factors;
- **bacterial diseases**, including those arising from antimicrobial resistance, since treatment methods exist (though bacterial co-infections are included in our estimates of direct deaths for viral respiratory diseases);
- **other non-viral diseases** (e.g., prions and fungi), since their geographies, modes of transmission, and transmission efficiency are limited; and
- **"unknown unknowns"**: diseases caused by pathogens not thought to have the potential to infect humans, or those wholly unknown to science.[1]

....

1   It is important to bear fully in mind the significance of unknown unknowns; after all it is not so very long ago that HIV/AIDS would have fallen into this category.

We also do not model risk from bio-terror (deliberate release of infectious agents) or bio-error (accidental release of infectious agents, for example from laboratory accidents), as this would require additional modeling efforts incorporating, for example, the characteristics, capabilities, and strategies of terrorist organizations, and biosafety protocols and practices within specific laboratories. These factors can be explicitly modeled and linked with the broader risk modeling framework that we present here, but are beyond the scope of our present analysis.

While epidemics can lead to many adverse outcomes—including infections, hospitalizations, deaths, societal disruption, educational delays, and economic shocks—in this chapter we focus on deaths. We include neither morbidity estimates, nor estimates of the impacts of long-term sequelae, though these are important topics. The welfare losses caused by epidemics and pandemics—including economic damages (see Fan et al., 2017) as well as losses to education, livelihoods, and trauma and psychological damages—are considerable, but require distinct modeling techniques and are beyond the scope of this chapter. We focus on deaths in this chapter as they are the most readily measurable, observable, and reported metric, and therefore provide a less biased indicator of epidemic severity than other metrics such as infections or hospitalizations.

Given all of the above considerations, the estimates we present in this chapter are not intended to capture the totality of epidemic risk. Rather, they should be interpreted as a lower-bound estimate of the potential loss from such events.

TABLE 1. Key Terms and abbreviations

Term	Definition Used in This Chapter
Average annual loss (AAL)	The expected loss (in this chapter, deaths) per year. Further details on its calculation are provided in Annex A.
COVID-19	A coronavirus pandemic caused by SARS-CoV-2, beginning in 2019.
Direct mortality (or direct deaths)	Deaths caused by primary infection with a pathogen and any immediate secondary effects resulting directly from that infection. We measure direct mortality from the time when an epidemic begins to when transmission ceases.
Epidemic	"The occurrence in a community or region of cases of an illness … clearly in excess of normal expectancy" (Porta, 2014).
Event catalog	A collection of historical or modeled events and associated data on event parameters and outcome estimates (Madhav et al., 2021).

TABLE 1. (Continued)

Term	Definition Used in This Chapter
Exceedance probability function (EPF), annual	A function, also known as an "EP curve", which provides the probability that an event of a given severity or worse will begin within a given year. For the purposes of this chapter, severity is measured in terms of deaths.
Excess mortality (or excess deaths)	"The mortality above what would be expected based on the non-crisis mortality rate in the population of interest" (WHO, 2022a).
Normalized deaths	Deaths per 10,000 population. Also referred to in this chapter as population normalized deaths.
Pandemic	"An epidemic occurring over a very wide area, crossing international boundaries, and usually affecting a large number of people" (Porta, 2014). In this chapter, when we refer to epidemics this includes pandemics as well. That is, all pandemics are epidemics, but not all epidemics reach the level of becoming pandemics.
Respiratory diseases	Diseases that affect the lungs and other parts of the respiratory system (NCI, 2023). Respiratory diseases of pandemic potential constitute one of the two disease categories modeled in this chapter. The modeled pathogens include pandemic influenza and novel/epidemic coronaviruses.
Return period	Inverse of annual exceedance probability; Average time between events of a given magnitude or greater (Box 1). Also known as return time or recurrence interval.
Risk	The quantitative combination of the following information: (1) what can occur, (2) the probability that it can occur, and (3) the potential magnitude of consequences that can result (Kaplan & Garrick, 1981).
Zoonotic spillover (or "spark") risk	Risk of transmission of an animal pathogen to a human (See "zoonotic pathogen", defined below).
Spread risk	Risk that a pathogen spreads from person to person.
Tail risk	Risk of low-probability, high-impact events (Cirillo & Taleb, 2020).
Viral hemorrhagic fevers (VHFs)	Diseases caused by viruses that damage organ systems, leading to hemorrhaging (CDC, 2021). VHF epidemics constitute one of the two disease categories of events modeled in this chapter. The modeled pathogens include Ebola, Marburg, and Nipah viruses.
Zoonotic pathogen	"An infectious pathogen or parasite that originates in (or is maintained in the wild by) one or more non-human hosts, but can be transmitted to and cause disease in humans" (Han et al., 2016). The process by which a zoonotic pathogen is transmitted to a human being is called "zoonotic spillover."

BOX 1. Rolling the dice

Mathematically, the return period is the inverse of the exceedance probability (EP) (Table 1). For example, a 1% annual exceedance probability—a 1 percent chance of observing an event of a given severity (or worse) in a year—translates to a 100-year return period, or alternatively, a "1-in-100 year event" (FEMA, 2016). While the return period is a convenient way to conceptualize the estimates we present in this chapter, this can also lead to misinterpretation of the level of risk. This type of misinterpretation can cause decision makers to underinvest in preparing for low probability, high severity events, by assuming (implicitly or explicitly) that the risk is "tomorrow's problem."

It is all too easy for even informed analysts to misinterpret frequency estimates for rare events. A 100-year return period does not mean that the level of loss occurs once per 100 years, nor does it mean that the losses are evenly spaced out at 100 year intervals. A "1-in-100 year event" simply means the event statistically has a 1% chance of starting in any given year. This means that a given event is expected to occur, on average, once in repeated samples of 100 year time periods. It is even possible to have multiple "100-year" events occur during a 100-year period.

With this in mind, any given year is a roll of the dice.

Drivers of epidemic risk

Risk modeling is not simply an exercise in mathematics—it must appropriately represent real-world processes, and modelers should have familiarity with the complex web of underlying factors shaping the risk. Our modeling framework therefore explicitly incorporates several critical drivers of epidemic risk, including zoonotic spillover, global travel patterns, and governance challenges. Here we provide background information about these processes; specific details of how they are incorporated into our models are provided in Annex A.

Nearly all modern pandemics have sparked when zoonotic pathogens have jumped from animals to humans, often through activities such as hunting, habitat encroachment, and intensive livestock farming (Jones et al., 2013; Olival et al., 2017). Multiple studies have shown that epidemics, especially those caused by zoonotic spillover events, are increasing in both frequency and severity (Jones et al., 2008; Smith et al., 2014). For a subset of high priority viruses, this trend is exponential, meaning that not only are epidemics becoming more frequent and more severe but that spillover-driven epidemics are occurring at an accelerating rate (Meadows et al., 2023). Climate change and other forms of anthropogenic environmental change, such as deforestation and habitat fragmentation, are predicted to increase the frequency of zoonotic spillover events because they increase the frequency of contact between humans and animal reservoir species (Carlson et al., 2022).

Increasing human population density and connectivity through global travel and trade facilitate the spread of the outbreaks (Baker et al., 2021). The accessibility of global air travel makes effective containment of emerging outbreaks increasingly difficult because infected individuals can disperse over large geographic distances before cases are detected and reported to public health officials (Meslé et al., 2022). For example, rapid geographical spread was well-documented in the severe acute respiratory syndrome (SARS; caused by SARS-CoV-1) outbreak of 2003. One individual infected ten people in a Hong Kong hotel, six of whom took international flights to Australia, Canada, Singapore, the Philippines, and Vietnam. These traveling secondary cases subsequently led to SARS outbreaks in Hanoi, Singapore, and Toronto within a few days of the first reported case in Hong Kong (Cherry, 2004). Similarly, during the COVID-19 pandemic, early detection of SARS-CoV-2 variants occurred in airline passengers (Wegrzyn et al., 2022). Spread by air travel also occurred during the 2014 West Africa Ebola epidemic (Gomes et al., 2014).

Experience in infectious disease crises, such as COVID-19 and the 2018 North Kivu Ebola virus epidemic, has provided a clear reminder that governance and human behavior play important roles in shaping infectious disease transmission. Research on the relationship between governance and epidemic risk suggests that political factors also play an important and underappreciated role in both frequency and severity of epidemics. Armed conflict and political instability can degrade disease surveillance systems, creating "blind spots" and lengthening the period during which disease transmission can occur before it is detected and mitigation measures are put in place (Wise & Barry, 2017). These same factors can also increase the risk of disease spread by facilitating population displacement (Price-Smith, 2001). Public distrust of government institutions can also impede disease control measures, potentially leading to increased morbidity and mortality (Vinck et al., 2019; Bargain & Aminjonov, 2020; Farzanegan & Hofmann, 2022).

Techniques for estimating risk

Apart from research published in DCP-3, there is scant scientific literature dedicated to estimating the frequency and severity of infrequent, high-consequence epidemics (Fan et al., 2017; Madhav et al., 2017). Methods for estimating risk and burden of endemic and frequently-occurring diseases are well-described; however, the quantification of risk—especially tail risk—from more sporadically-occurring epidemics is not explored in major public health or infectious disease epidemiology textbooks (Bennett et al., 2019; Nelson & Williams, 2014). Contributions on this topic have instead come from interdisciplinary research teams or the private sector (Cirillo & Taleb, 2020; Marani et al., 2021; Wilkinson, 2021). The relatively limited public health literature on the prospective analysis of risk and burden posed by epidemics is perhaps attributable to the multidisciplinary nature of the problem, and the development of estimation techniques within fields that have had limited interaction with public health researchers.

Following the conventions from DCP-3, this chapter provides risk estimates in the form of exceedance probability functions (EPFs; Table 1) (Madhav et al., 2017). An EPF can be analyzed to estimate the probability that an event of a given severity or worse will start in a given year, and other metrics of interest, such as the average annual loss (AAL; Table 1).

Modelers can estimate EPFs using empirical data from historical events, or use simulated data from modeled events. Empirical EPFs derived from historical data are most appropriate for pathogens that cause frequent outbreaks, or have a recurrent or seasonal pattern (for example, seasonal influenza or meningococcal meningitis). A historically-derived empirical EPF may be misleading where historical data is sparse, marked by underreporting, or includes unincorporated trends that could influence future expected losses (Madhav et al., 2021). For these reasons, we generate EPFs using a probabilistic modeling approach that generates an event catalog (Table 1) containing simulated events.

Historical data analysis

Historical data are often the first point of reference for evaluating future risk. While historical data can offer valuable insights, constructing a view of future risk based on empirical data can be misleading, especially for infrequent events. In this section we highlight the factors that can make historical data an unreliable indicator of future risk, which demonstrates why we take an extreme events modeling approach to quantify the risk.

Figure 1 shows a hypothetical time series of historical data. In the graph, it is possible to see the differences between endemic disease patterns as compared to pandemic disease patterns. In this hypothetical 360 weeks—roughly seven years—of data, the endemic disease occurs regularly throughout this time period in a relatively well-characterized pattern. This is in contrast to a pandemic event, which occurs in a single spike spanning approximately one year. Interestingly, in this graph, both the endemic disease and the pandemic disease actually have a similar AAL, but have very different characteristics of frequency and severity that lead to those annual average values.

FIGURE 1. Example comparison of timing and magnitude of endemic vs. pandemic deaths
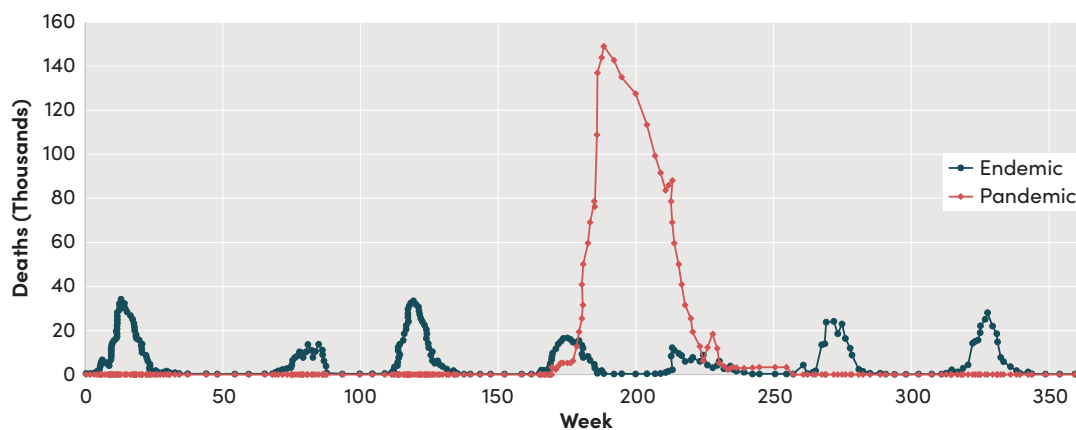
For frequently-occurring infectious diseases having well-characterized historical patterns, historical data can yield acceptable estimates of future risk. This is somewhat true for the historical record on pandemic influenza which, while having important limitations, does provide evidence of several major events per century (Morens et al., 2010). Historical data analysis can reveal changes over time, such as increasing frequency and severity of events, rate of increase, and factors that drive this dynamic (Meadows et al., 2023). Techniques for estimating risk based solely on historical data include, for example, statistical and actuarial modeling and parametric curve fitting (Embrechts et al., 1999).

However, the historical record represents only a small subset of the possible events that can occur, especially for low probability, high severity events. It therefore represents a limited sample size, which can lead to erroneous conclusions about what could occur in the future (Box 2). The absence of empirical data in the form of observed events can be mitigated somewhat by considering counterfactual events (Resolve To Save Lives, 2021), but this does not necessarily provide information about how severe an event would have been if it had occurred. Pandemics are relatively rare, and there are large variations in severity. For example, consider the vast difference in mortality between the 1918 and 2009 influenza pandemics.

BOX 2. The importance of tail risk

The severity distribution of epidemics is highly skewed, exhibiting a very long "tail", consisting of very rare, severe events. When there is a small sample of data points (in this case, historical events) from a highly skewed distribution, the "heaviness" of the tail is often underestimated. This is problematic, as an accurate understanding of expected losses—especially those caused by less frequent, highly damaging events—is needed to appropriately plan for future events.

Figure 2 shows the distribution of cases from historical filovirus events (Meadows et al., 2023), and how the fitted distribution changes over time as more events are added. As more events occur over time, the tail of the distribution (defined as the upper 1%) gets longer and heavier, which shifts the expected value (mean) of the distribution as well as the range and expected value of the tail, to the right. There are two explanations for this finding: 1) as the sample size increases over time, the sample distribution and mean get closer to the true distribution, or 2) the true distribution is becoming more skewed over time, meaning events are getting more severe. The true cause is likely a combination of these two factors.

The estimation of tail risk affects decision makers' preparedness planning. When they have limited resources and need to directly weigh epidemic impact against other health risks, properly accounted-for tail risk is critical to understanding the expected value of future losses. In addition, carefully quantifying tail risk can help planners assess and properly plan for low frequency, high severity events. By using epidemiological data and computational modeling, it is possible to supplement historical data with simulated events. These simulations can then provide additional data points on which to base the distribution, and allow for a more robust estimation of the tail.

FIGURE 2. Distributions of historical filovirus cases per outbreak over time showing the fitted probability density function (red line)
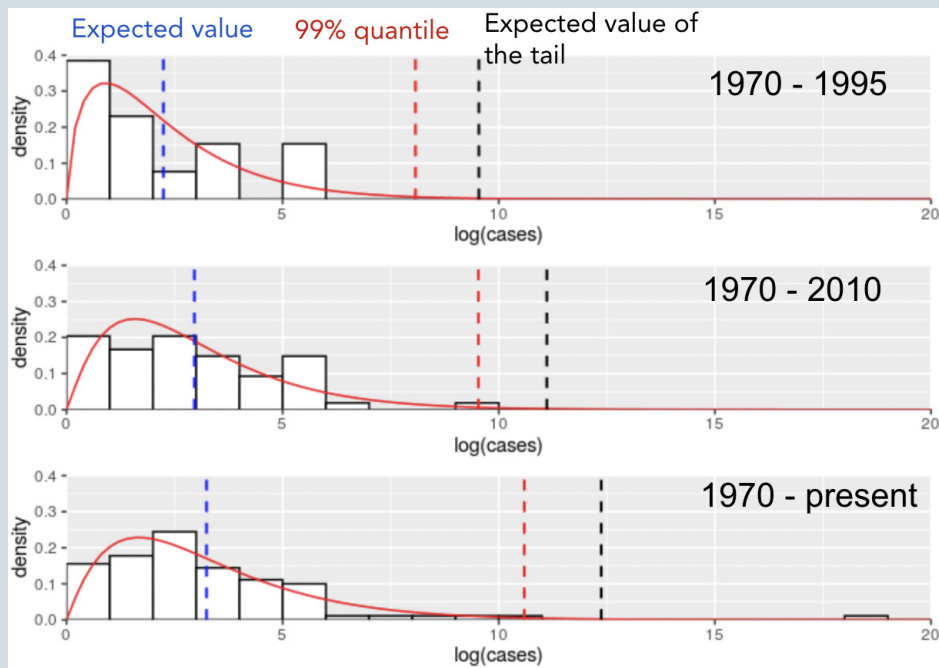
Notes relating to Figure 2: The x-axis shows a log base 10 transformation of the number of cases. The "tail" is defined as the upper 1% of the probability density function.

Constructing a historical view of epidemic risk is further complicated by the many challenges and biases found in reported epidemiological statistics (Badker et al., 2021). These factors can lead to data inconsistencies and lack of comparability across different information sources, which further compounds the uncertainty in these estimates. These challenges can be found in all types of epidemic data, including for both respiratory and VHF events.

In addition to data challenges, many diseases are underreported, leading to biased estimates of severity, which is particularly problematic in resource-limited settings (Glennon et al., 2019). Underreporting is driven by many factors including disease symptomology and severity, contextual conditions (such as local clinical capacity), which can influence mortality rates, public health and disease surveillance infrastructure, socio–cultural factors (such as stigma attaching to particular symptoms or diseases), and government censorship (Meadows et al., 2022).

Extreme events modeling

Extreme events (or "catastrophe") modeling can overcome the challenges of using historical data to develop risk estimates for infrequent, high severity events, known as "tail risk" (Box 2) (Cirillo & Taleb, 2020). For example, the (re)insurance industry routinely consults with modeling experts in natural hazard fields such as meteorology, seismology, hydrology, and volcanology for this purpose (Kozlowski & Mathewson, 1995). However, these extreme events modeling techniques tend to be

taught within, and utilized by, intellectual communities that have limited cross-pollination with public health actors.

Extreme event modeling techniques build on historical data as a starting point, and use extensive mechanistic modeling and simulation to fill in the gaps beyond the available historical data. The extreme events modeling framework also enables analysts to assess the influence of inputs that may not exist in the historical record, but are biologically and epidemiologically plausible. For example, even if a vaccine or treatment option has not yet been widely used but could potentially be deployed in reaction to an outbreak, simulation models can include this treatment where appropriate.

Where extreme event modeling techniques are applicable, there are still substantial technical and analytical requirements for this modeling approach to be effectively utilized. Extreme event models typically require significant computational infrastructure and resources, have many parameters to estimate, and for epidemics (unlike for natural hazards) must account for the effects of human behavior in shaping the course of events.

Methods used in this chapter

Risk estimation process

The risk modeling approach we use to develop the estimates in this chapter draws from principles in computational epidemiology, social science, extreme events modeling, actuarial science, and other fields to produce millions of simulated epidemics and pandemics. Our process requires us to develop probability distributions for each model parameter, statistically sample values from these parameter distributions, seed each simulation with these parameter values as initial conditions, and then simulate the spatio-temporal spread of the events through a global, stochastic, metapopulation disease spread model that incorporates information about population vulnerability, mobility patterns, medical technology, preparedness levels, and intervention measures. Comprehensive details of our methods are provided in Annex A of this chapter.

We consider an event to be active in our simulations until transmission ceases, whether through stochastic die-off, herd immunity, non-pharmaceutical interventions, or other phenomena. We include only the acute portion of the events, and do not include any transition to an endemic state. We make this assumption due to the lack of consistent epidemiological standards to select cutoff points indicating the transition from epidemic to endemic state. As a result, our loss estimates represent a lower bound; they do not capture ongoing mortality from endemic transitions, in which a pathogen enters a seasonal or cyclic pattern with an ongoing and persistent mortality burden, as occurred during the 1918 influenza (Taubenberger & Morens, 2006) and the COVID-19 pandemics (Contreras et al., 2023).

Our simulation process results in model event catalogs (Table 1), each containing 100,000 simulated years and encompassing millions of infectious disease scenarios, which we use to estimate the risk

from epidemics. It should be noted that our event catalogs do not project 100,000 years into the future, but rather, represent 100,000 versions of "next year." We generate these catalogs separately for both respiratory diseases and viral hemorrhagic fevers (VHFs) (Table 1), and our results are also divided in this way. We do this for ease of interpretation, because deaths from respiratory diseases comprise the vast majority of expected deaths from the epidemics that we have modeled. There are orders of magnitude of difference between the levels of potential losses caused by these disease categories, and combining them would obscure this asymmetry. Additionally, different types of response measures may be more relevant and cost-effective for combating each disease category, which is easier to tease apart when loss estimates are separated.

We use these event catalogs to produce several estimates, including average annual loss (AAL, measured in deaths), population normalized deaths, exceedance probabilities (EPs), and age- and region-specific mortality estimates (region definitions shown in Figure 3 and Annex B). The AAL estimates—expected value of annual losses—are shown as normalized deaths per 10,000 population and deaths in thousands. Population numbers are from the UN Population Division's World Population Prospects 2022 release, using a reference year of 2020, for a total estimated global population of 7.8 billion (United Nations Population Division, 2022).

In addition to annual estimates, we also estimate cumulative exceedance probabilities (CEPs) over periods of y years using the formula

$$CEP = 1 - (1 - EP)^y$$

where y is the time horizon of interest. In this chapter, the time periods of interest are 5, 10, and 25 years; however, the CEP can be computed over any potential time period of interest (for example, over the lifetime of a person born next year and expected to live to the current global life expectancy of approximately 73 years). The CEP is thus another, potentially more useful, way of conveying the same information as the annual EP estimates. It demonstrates the potentially large cumulative risk posed by rare events and estimates risk for time durations of greater interest to policymakers.

Our CEP estimates contain significant assumptions, but likely represent a reasonable lower bound for medium-term pandemic risk. The CEP formula assumes that the risk remains constant at current levels and each year of the time period is independent. Our CEP estimates therefore assume that there are no changes to underlying drivers of risk that could impact the frequency and severity of future epidemics. However, current trends suggest that infectious disease risk is increasing (Meadows et al., 2023), driven by increasing human-wildlife contact, deforestation, urbanization, intensifying demand for animal protein, and intensifying international travel (Baker et al., 2021; Carlson et al., 2022). Our estimates likewise do not incorporate assumptions about the potential beneficial impact of new vaccine platforms, improvements to global infectious disease surveillance, early warning, and preparedness. On balance, though, the risk is probably higher over the medium term future than our assumption of constant risk implies.

Direct deaths vs. excess mortality

The modeled deaths we present in this chapter are total direct deaths, rather than reported deaths or excess deaths. We consider direct epidemic deaths to be those caused directly by primary infection with the pathogen and any immediate secondary effects resulting directly from that infection (e.g., pneumonia resulting from infection with pandemic influenza).

It is important to be explicit about what we count as a direct death in this chapter. We adopt nomenclature from WHO's assessment of the number of deaths associated with COVID-19 (Msemburi et al., 2023). WHO begins with the concept of "excess deaths" which is defined as the differences between an estimate of actual deaths in the period under consideration and an estimate of what the number of deaths would have been, had past trends continued. WHO's COVID-19 excess mortality estimates were calculated by taking the difference between observed all cause mortality and expected mortality in 2020–2021. Expected mortality was modeled by projecting monthly all cause mortality data from 2015–2019 to 2021. Msemburi and colleagues estimate global excess deaths in the COVID-19 years of 2020 and 2021 to have been 14.8 million, which is 2.7 times the 5.42 million reported global deaths from COVID-19 during that same time period (Table 2; regional groupings provided in Figure 3 and Annex B). They partition these excess deaths into 4 categories:

A. strictly non-COVID-19 deaths (e.g., from other external events such as wars or natural disasters);
B. indirect COVID-19 deaths (e.g., deaths occurring from health system overload);
C. direct COVID-19 deaths that were not reported; and
D. direct COVID-19 deaths that were reported (5.42 million).

The excess mortality estimates also account for any deaths that were averted due to pandemic-related changes in social conditions and personal behaviors (e.g., fewer traffic deaths due to reduction in travel and working from home or fewer influenza deaths due to COVID-19 mitigation strategies such as masking and stay-at-home orders). In some countries (e.g., China, New Zealand, Australia, and Japan), it was estimated that a higher number of deaths were averted due to pandemic-related behavioral changes than were directly or indirectly attributable to COVID-19, resulting in a net negative excess mortality during the 2020–2021 study time period. However, substantial changes in disease control policies and disease transmission from 2022 onward led to substantial increases in mortality; incorporating data from this time period could substantially alter the understanding of the regional distribution of excess mortality from COVID-19.

The WHO analysis attempts no estimate of the division of the 9.4 million excess deaths not reported as COVID-19 deaths (14.8 million—5.4 million) among the categories (A), (B) and (C). But the paper does observe that "…the greater proportion of excess deaths can be attributed to COVID-19 directly."

The risk modeling results we provide in this chapter include both reported and unreported direct deaths; that is, they represent the sum of categories (C) and (D) described above. While WHO does

not report that sum directly, a number consistent with their paper would be 11—12 million direct COVID-19 deaths in 2020–21.

TABLE 2. Excess deaths and reported COVID-19 death totals for January 2020–December 2021 by region[1]

Region[2]	Excess Deaths per 10,000 Population (WHO Modeled) (Msemburi et al., 2023)	Reported Deaths per 10,000 Population (WHO, 2022b)	Excess to Reported Death Multiplier
Global	19	7.0	2.7
India	34	3.4	10
Sub-Saharan Africa	11	1.3	8.5
Central Asia	14	2	7
Western Pacific and Asia	12	3.4	3.5
Middle East and North Africa	19	6.6	2.9
Central and Eastern Europe	59	24	2.58
Latin America and Caribbean	35	24	1.5
North Atlantic	22	20	1.1
China[3]	−0.37	0.04	−9.2

Notes:

1. The numbers in this table are rounded to two significant digits;
2. Regional groupings provided in Figure 3 and Annex B;
3. Excess mortality in China greatly increased in December 2022 (after the timeframe of the analysis) following decisions to end a national policy that incorporated extensive testing and non-pharmaceutical interventions to reduce transmission; excess deaths for the entirety of the pandemic would be substantially higher than these estimates.

FIGURE 3. Regional grouping of countries

- Central and Eastern Europe
- Central Asia
- China
- India
- Latin America and Caribbean
- Middle East and North Africa
- North Atlantic
- Sub-Saharan Africa
- Western Pacific and Asia
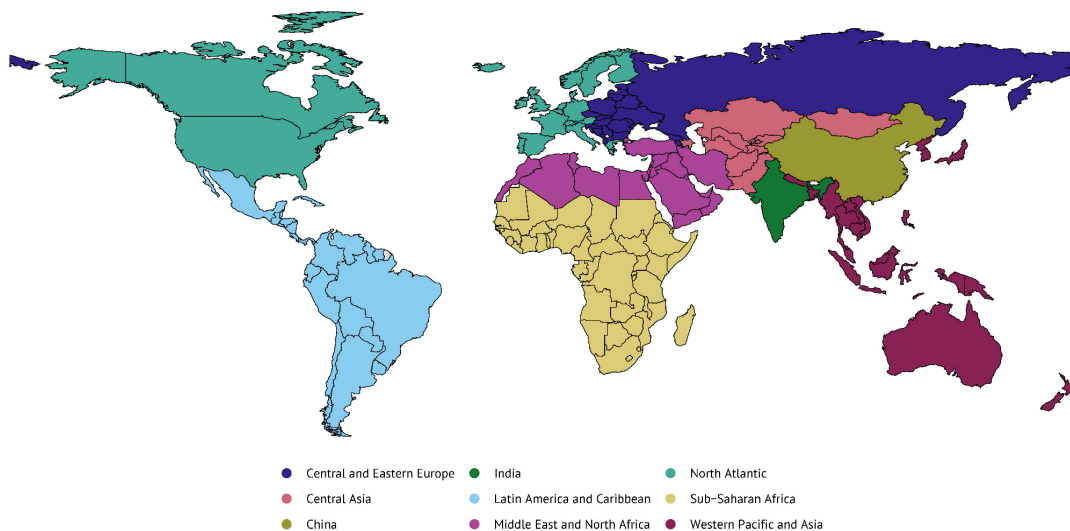
Notes pertaining to Figure 3: This grouping is used in DCP-4, Volume 2 and by the Lancet Commission on Investing in Health. Annex B lists the countries in each region. This grouping may be subject to change in future revisions of this paper.

Limitations & uncertainty in model estimates

Models are abstractions of the real world. Therefore, there are by necessity some limitations of the approach we have taken. First, historic data are limited; and though we have taken great care to mitigate this with the modeling approach, it is not possible to fully account for gaps and biases in historical data. Second, there are many parameters to estimate, all of which have substantial uncertainty. Third, the outcomes of pandemics are affected by human behavior and movement patterns, which can vary substantially in specific socio-economic contexts and subpopulations, or could change over time in surprising ways that may not be fully accounted for or characterized in the model. Fourth, models do not fully account for secular trends such as the apparent increase in zoonotic spillover events that can spark pandemics, or amplification patterns that could arise from the intersection of trends in spillover with the intensification of climate change.

It is worth emphasizing that although we have performed extensive model diagnostics and validation—including sensitivity analyses, benchmarking of historical events, and cross-referencing against other data sources—substantial uncertainty attaches to our estimates. This uncertainty results in part from the historically-informed probability distributions from which we draw key parameters for our simulations. Additionally, substantial uncertainties exist in the underlying structure of our models and factors that might influence the future evolution of parameters in ways poorly reflected in history. Further discussion of uncertainty can be found in Annex A.

In this chapter we estimate 95% confidence intervals for deaths by sampling one thousand subsets of 10,000-years each from the broader 100,000-year model event catalogs and estimating the 2.5% and 97.5% percentiles from the samples. As such, the confidence intervals (CIs) convey the uncertainty in catalog sampling, rather than the full universe of uncertainty.

Because of the relatively small width of our estimated CIs for the AAL estimates, and the larger uncertainties that surround the analysis, we do not report CIs for the AAL, as this has the potential for conveying false precision.

We have calculated CIs associated with our EP estimates; these CIs typically fall in the range of 5–20% of estimated values, and expand to 40% or more of estimated values as one goes further into the tail of the EPF. It is an important feature of the EPF that the confidence intervals widen markedly as one moves further out in the tail of the curve. This is expected; estimates for extremely rare, massive pandemics are inherently uncertain, given their sparsity.

Further uncertainty is found in the extreme tail of the EPF, due to our models, assumptions regarding socio-behavioral responses during epidemics. These assumptions might not hold true under extreme, high severity scenarios. For example, in a truly massive event, there could potentially be very intense governmental and societal responses to curtail transmission. Major social change could occur (e.g., mass quarantine, or compulsory licenses of vaccine intellectual property), leading to better

outcomes than we estimate. Conversely, the possibility exists that during a truly massive pandemic, there could be a total societal collapse, which would lead to vastly worse outcomes than we estimate.

Our estimates—and in particular, estimates of risk decades into the future—should not be interpreted as conveying great precision, due to deep underlying uncertainties. Our headline numbers, rather, reflect broad ranges consistent with historical evidence and state-of-the-art modeling.

Results: respiratory diseases

Global respiratory mortality

We estimate the average annual loss (AAL) from future epidemics and pandemics caused by the modeled respiratory diseases to be approximately 2.5 million deaths. The AAL provides a summary measure of the scale of potential losses. Rather than representing the number of deaths that occur each year, the AAL arises from a pattern of events that exhibit larger amounts of deaths that occur more sporadically and in a punctuated manner (Figure 1). Within the respiratory event catalog, pandemic influenza viruses are the predominant contributors to the losses, contributing nearly twice as much to the AAL in comparison to epidemic/novel coronaviruses (Table 3).

TABLE 3. Global average annual deaths based on respiratory model event catalog

	Average Annual Deaths	
	Counts (Thousands)	Per 10,000 Population
Pandemic influenza	1,600	2.0
Epidemic/novel coronaviruses	890	1.1
Total	2,500	3.2

An inspection of the EPF (Table 4, Figure 4) shows a heavily skewed (i.e., asymmetrically overdispersed) distribution of loss estimates. Smaller events are more likely to occur, but larger events—even larger than those historically observed—are also possible and represented further out in the tail of the distribution. As the probability decreases (or return period increases), there is an initial, rapid increase in the number of deaths, which decelerates as one moves further into the tail of the distribution. The steep rise in event severity is apparent in the higher-frequency (i.e., lower return period) portion of the curve, perhaps most visibly in the large jump in the number of deaths between the 10- and 20-year return periods. While the steepness of the rise decreases further out in the tail, the tail events contribute substantially to the skewness of the distribution (Box 2). The steep rise and heavy tail of the curve are consistent with the potential for wide transmission and global spread of respiratory diseases.

TABLE 4. Selected exceedance probabilities and associated global deaths based on respiratory event catalog

Return Period	Exceedance Probability	Deaths per 10,000 Population (95% Conf. Int)	Death Counts (Thousands) (95% Conf. Int)
5	0.20000	0.001 (0.001, 0.001)	0.53 (0.50, 0.55)
10	0.10000	0.002 (0.002, 0.002)	1.4 (1.2, 1.5)
20	0.05000	7.2 (5.4, 10)	5,600 (4,300, 7,700)
35	0.02857	28 (23, 32)	22,000 (18,000, 25,000)
50	0.02000	45 (39, 53)	35,000 (30,000, 42,000)
100	0.01000	86 (74, 100)	68,000 (58,000, 80,000)
200	0.00500	150 (120, 180)	110,000 (100,000, 140,000)
333	0.00300	200 (160, 220)	150,000 (130,000, 170,000)
500	0.00200	220 (200, 260)	170,000 (150,000, 200,000)
667	0.00150	250 (210, 290)	190,000 (170,000, 220,000)
1000	0.00100	280 (240, 390)	220,000 (190,000, 300,000)

FIGURE 4. Global respiratory exceedance probability function
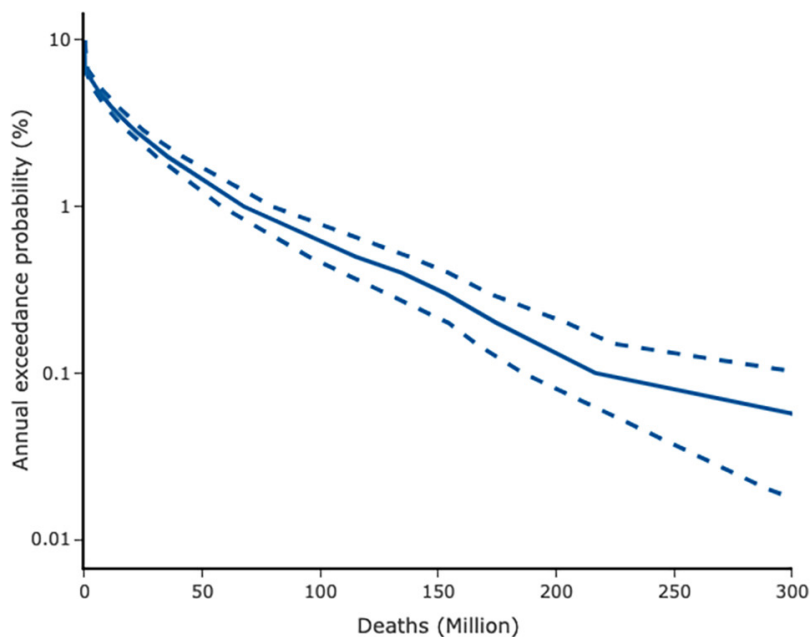
We also used the EPF to estimate the level of mortality found at different EPs (Table 5), and to take an in-depth look at the likelihood of an event having mortality of a comparable magnitude to the COVID-19 pandemic (Box 3).

TABLE 5. Exceedance probabilities for selected global death levels based on respiratory event catalog

Global Severity		Likelihood	
Death Counts	Deaths per 10,000 Population	Return Period	Exceedance Probability
>800	>0.001	7	14%
>80,000	>0.01	15	6.8%
>8,000,000	>10	22	4.5%
>80,000,000	>100	120	0.8%

BOX 3. COVID-19 is not a "once in a century pandemic"

The panic and neglect cycle is driven, at least in part, by the historic fact that severe pandemics occur infrequently. While the 21st century has seen multiple pandemics—including the 2009 pandemic influenza and Zika virus—the last public health crisis seemingly comparable in impact to COVID-19 was the "Great Influenza" of 1918 (Johnson & Mueller, 2002). Since COVID-19 occurred nearly 100 years after the 1918 pandemic, some commentators have described pandemics of this scale as occurring "once in a lifetime" (Guterres, 2020) or even "once in a century" (Cruickshank & Shaban, 2020; Gates, 2020; WHO, 2020).

At the end of December 2022—the end of the third year of the pandemic—there were over 660 million reported cases and 6.5 million reported deaths globally from COVID-19 (Ginkgo Bioworks, 2023). Based on our simulated event catalog, we estimate the annual probability of an event of this magnitude or larger to be 0.02–0.03. In other words, every year there is a 2–3% chance that an event equal to or more severe than COVID-19 (in terms of mortality) could occur. Expressed in terms of return periods, this would be a 33–50 year event, rather than a 100 year event. Assuming that the level of risk does not change, we further estimate that there is a 10–14% chance (cumulative exceedance probability) of an event as severe as or worse than COVID-19 occurring over the next five years, an 18–26% chance over the next decade, and a 40–53% chance over the next 25 years.

COVID-19 was more severe than other recent respiratory pandemics, such as the 1957, 1968, and 2009 influenza pandemics. However, comparing COVID-19 to the 1918 Influenza pandemic, as many have recently done, sets up a false equivalency. As Table A.13 (see Annex A) shows, as a percent of global population mortality the 1918 pandemic was orders of magnitude more severe than COVID-19, as it led to the deaths of up to 5% of the global population; compare this to the estimated 0.08% global mortality from COVID-19 as of December 2022, based on reported deaths.

Our estimates of the frequency and severity of pandemics, rooted in extreme events modeling techniques, demonstrate that COVID-19 is not likely to be a "once in a century" pandemic. To the contrary, over the next 25 years, we estimate that a pandemic with magnitude similar to or worse than COVID-19 has a roughly 50% probability of occurrence, similar to flipping a coin.

Because severe respiratory pandemics occur sporadically and have a relatively low (perceived) probability of occurrence in any given year, policymakers tend to underinvest in preparedness (Sands et al., 2016). Viewed over a time-horizon that is longer—but still relevant to policymakers and planners—the substantial magnitude of the risk from rare, potentially catastrophic events becomes more apparent (Table 6). For example, we estimate that the annual probability of a respiratory pandemic killing at least 10 million people worldwide is 4.2%; yet, over a 10 year period, the probability of such an event occurring is 35%. Extrapolated further, our results suggest that over the next 25 years, there is a 66% probability of a respiratory pandemic that would kill 10 million people or more, with the caveat that many of the assumptions in our risk modeling approach have greater uncertainty over a longer time period.

TABLE 6. Annual, 5 year, 10 year, and 25 year exceedance probability (EP) estimates for selected global event sizes based on the respiratory event catalog

Deaths	Annual EP	5 Year EP	10 Year EP	25 Year EP
1,000,000	6.3%	28%	48%	80%
10,000,000	4.2%	19%	35%	66%
100,000,000	0.6%	3.0%	5.8%	14%

Although the respiratory model event catalog contains a wide range of event sizes, we estimate that the vast majority of the risk from respiratory disease pandemics is in the tail of the EPF: low probability, high impact events. Approximately 50% of the simulated events in the catalog are very small, with an average magnitude of 120 global deaths. Roughly 4% of events have 8 million or more global deaths. Only 0.6% of events have global death tolls exceeding 100 million. It is striking, however, that the comparatively small number of high-magnitude events heavily drive the estimates of expected mortality. The 1.4% of catalog events with death totals exceeding 50 million comprise 68% of all deaths in the respiratory catalog (Figure 5, Table 7). Although the higher-frequency events (≤35 yr RP) make the lowest contribution to AAL as measured in deaths (Table 7), these events can still cause substantial economic disruption (Madhav et al., 2017).

FIGURE 5. Respiratory catalog composition: simulated event sizes and their contribution to expected losses

Panel A: % of events

Event Size (Global Deaths)	%
200M+	0.14% Average deaths: 330M
(100M - 200M]	0.48% Average deaths: 140M
(50M - 100M]	0.8% Average deaths: 70M
(8M - 50M]	3.1% Average deaths: 23M
(80K - 8M]	2.3% Average deaths: 3.4M
(600 - 80K]	11% Average deaths: 2.0k
(200 - 600]	31% Average deaths: 330
[0 - 200]	51% Average deaths: 120

Panel B: % of deaths

Event Size (Global Deaths)	%
200M+	18% Average deaths: 330M
(100M - 200M]	27% Average deaths: 140M
(50M - 100M]	23% Average deaths: 70M
(8M - 50M]	29% Average deaths: 23M
(80K - 8M]	3.1% Average deaths: 3.4M
(600 - 80K]	0.009% Average deaths: 2.0k
(200 - 600]	0.004% Average deaths: 330
[0 - 200]	0.003% Average deaths: 120

TABLE 7. Composition of average annual loss (AAL) for respiratory catalog by event severity and event frequency

AAL by Event Severity		AAL by Event Frequency	
Severity (Millions of Deaths Globally)	Contribution to AAL, Thousands (%)	Frequency Indicated by Return Period (Years)	Contribution to AAL, Thousands (%)
200+	450 (18%)	≤10	0.23 (0.01%)
100–200	670 (27%)	10–35	310 (13%)
50–100	560 (23%)	35–100	720 (29%)
8–50	720 (29%)	100–200	440 (18%)
<8	77 (3.1%)	200+	1,000 (40%)
Total	2,500 (100%)	Total	2,500 (100%)

Respiratory mortality by region

Respiratory diseases have a substantial expected impact on all geographies. However, risk is unevenly distributed (See Figure 3 and Annex B for detailed information on the regional country groupings). The highest normalized AAL is in Sub-Saharan Africa and lowest normalized AAL is in the North Atlantic region (Table 8, Figure 6).

TABLE 8. Average annual deaths by region based on respiratory model event catalog

Region	Average Annual Deaths per 10,000 Population (95% Conf. Int)	Average Annual Deaths (Thousands) (95% Conf. Int)
Global	3.2	2,500
Central and Eastern Europe	2.5	82
Central Asia	4.4	160
China	2.4	340
India	3.2	450
Latin America and Caribbean	2.8	180
Middle East and North Africa	3.0	160
North Atlantic	2.2	180
Sub-Saharan Africa	5.0	580
Western Pacific and Asia	3.0	340

FIGURE 6. Average annual respiratory disease deaths, by region
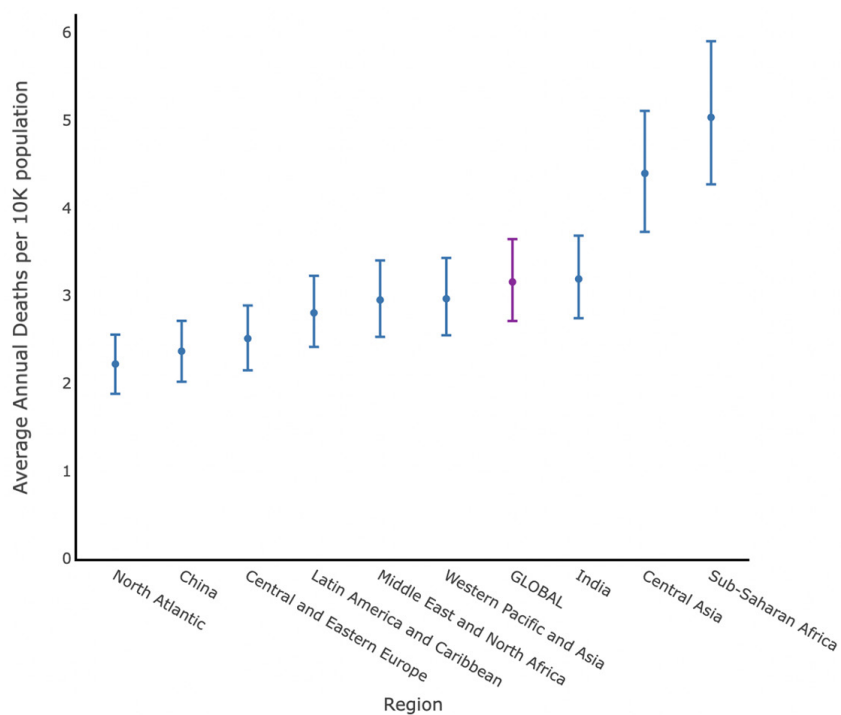
At first glance, our findings of higher expected mortality in Sub-Saharan Africa may appear inconsistent with the relatively low levels of reported mortality from the COVID-19 pandemic in Africa, as compared to other regions. Notably, the ratio of the population normalized AAL between Sub-Saharan Africa and the North Atlantic region as derived from Table 8 is roughly 2:1. This ratio is contrary to patterns of estimated excess mortality during the COVID-19 pandemic (Table 2), which shows higher mortality levels in the North Atlantic compared to Sub-Saharan Africa.

Multiple factors likely contribute to this apparent discrepancy. First, evidence suggests that there is significant underreporting in the official statistics—moreso in Sub-Saharan Africa than in the North Atlantic region. A higher mortality burden for Sub-Saharan Africa was found through estimates that draw on seroprevalence data to estimate mortality while correcting for underreporting (Kogan et al., 2022). Second, the age distribution of deaths is likely to play a role. Comparative mortality ratios show a much higher mortality burden for Sub-Saharan Africa, especially when accounting for the region's younger age distribution (Ledesma et al., 2023). Note that this could be a factor somewhat specific to COVID-19; a future respiratory pandemic could have a different pattern, potentially leading to a different spread in future expected losses. Third, mortality displacement may be playing a role. Both age effects and mortality displacement are discussed in the Respiratory Mortality by Age Group section, below.

Respiratory mortality by age group

AAL results by age group are also available in the respiratory model event catalog. Figure 7 shows a graph of the global normalized average annual deaths per 10,000 population by age group for respiratory pandemics. Table 9 contains the graphed values, including median and 95% confidence intervals for each age group.

These results show that members of the oldest two population groups are most likely to die during a respiratory pandemic, followed by the youngest in the population. The overall mortality rates exhibit a slight W-shaped pattern (Morens et al., 2021), although respiratory diseases can exhibit a number of different mortality patterns (for example U or J). The determinants of this pattern are not well understood, but may be related to immunity patterns in the population (van Wijhe et al., 2018).

Increased mortality, especially in older age groups, can lead to what is known as mortality displacement, or the "harvesting effect." When this occurs, there is a compensatory decrease in mortality after a pandemic, since the individuals who died in the pandemic would have been likely to die whether or not the pandemic occurred. This effect has been observed during influenza pandemics (Hoffman & Fox, 2019), as well as the COVID-19 pandemic (Astengo et al., 2021).

Beyond the oldest and youngest ages who are at greatest mortality risk during a respiratory pandemic, the age groups having the next greatest risk are the 20- to 39-year-old and 40- to 59-year-old categories. The increased mortality for the 20–39 age category is especially concerning from the standpoint of fertility, along with economic losses, as this age category includes prime members of the labor force who would be conducting economically productive activities. Therefore, epidemics having a W-shaped mortality pattern are more likely to cause the greatest economic loss (Ma et al., 2011).

FIGURE 7. Average annual respiratory disease deaths, by age group
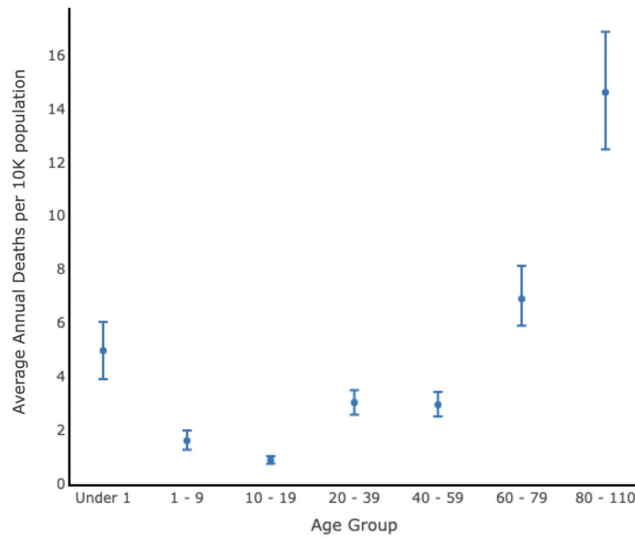
While the above results are averaged over the entire set of simulations, there are many potential forms that the age distribution can take for any single epidemic, and these may differ from distributions observed in previous epidemics. Illustrative examples of various age distributions are shown in Figure 8.

FIGURE 8. Illustrative respiratory disease age shapes
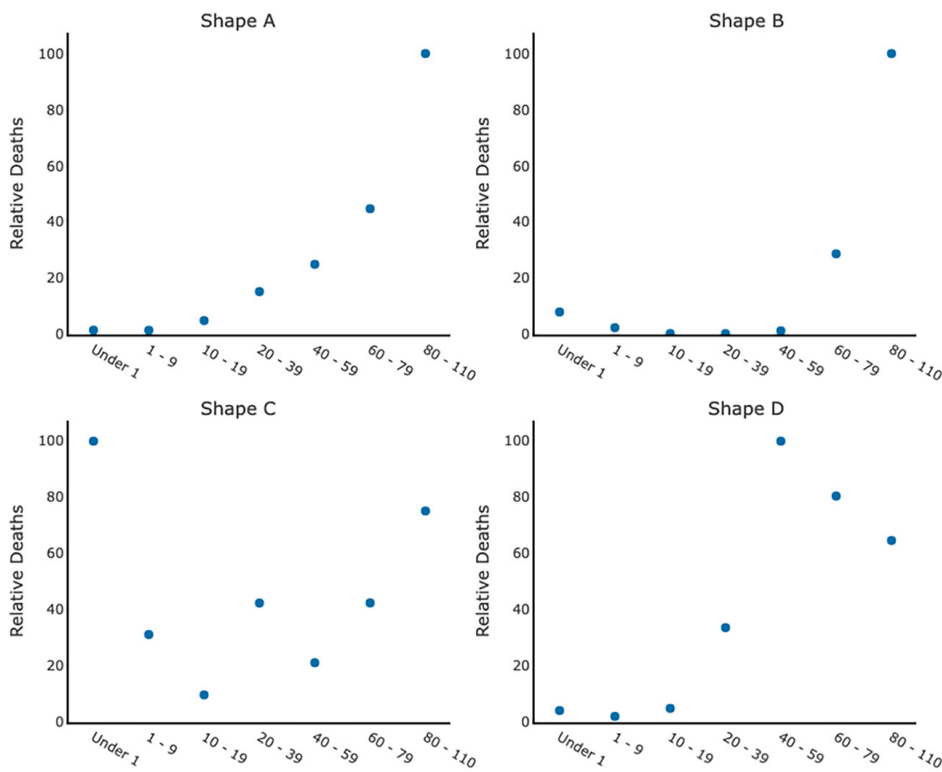
Note pertaining to Figure 8: Relative deaths represent the percent of normalized deaths in an age category compared to the age category having the highest normalized deaths.

TABLE 9. Global average annual deaths by age group based on respiratory model event catalog

Age Group (Years)	Average Annual Deaths per 10,000 Population in that Age Group (95% Conf. Int)	Average Annual Deaths in that Age Group (thousands) (95% Conf. Int)
Under 1	5.0	66
1–9	1.6	200
10–19	0.89	110
20–39	3.0	710
40–59	3.0	530
60–79	6.9	620
80–110	15	220
Global Total	3.2	2,500

Results: viral hemorrhagic fevers (VHFs)

VHF mortality in Sub-Saharan Africa

Viral hemorrhagic fevers (VHFs), such as those caused by Ebola, Marburg, and Nipah viruses, can be highly fatal, and human-to-human transmission can spark large, sustained epidemics. However, the severity of disease, distinctive signs and symptoms after the prodromal phase, and direct contact transmission mechanism all reduce the likelihood of wide international spread. Sub-Saharan Africa represents the vast majority of global VHF losses—approximately 72%. As such, we focus our analysis on this region. Sub-Saharan Africa regional estimates for the VHF catalog are presented below, including AALs and EPs.

We estimate the AAL from future VHF epidemics in Sub-Saharan Africa to be approximately 19,000 deaths (Table 10). This represents a small fraction of expected losses in comparison to respiratory pandemics. The EPF for VHFs exhibits a skewed distribution, though it is less skewed than the heavy-tailed loss distribution for respiratory diseases (Table 11, Figure 9).

TABLE 10. Sub-Saharan Africa average annual deaths based on VHF model event catalog

	Average Annual Deaths	
	Per 10,000 Population	Counts (Thousands)
Viral Hemorrhagic Fevers (VHFs)	0.17	19

TABLE 11. Sub-Saharan Africa deaths at selected exceedance probability points, based on VHF event catalog

Return Period	Exceedance Probability	Deaths per 10,000 Population (95% Conf. Int)	Death Counts, Thousands (95% Conf. Int)
5	0.20000	0.01 (0.01, 0.01)	1.3 (1.2, 1.4)
10	0.10000	0.06 (0.05, 0.06)	6.3 (5.6, 7.1)
20	0.05000	0.24 (0.21, 0.29)	28 (24, 33)
35	0.02857	0.69 (0.59, 0.85)	80 (67, 98)
50	0.02000	1.4 (1.1, 1.8)	160 (130, 210)
100	0.01000	4.2 (3.3, 5.3)	480 (380, 610)
200	0.00500	8.4 (6.7, 10)	970 (770, 1,200)
333	0.00300	12 (10, 15)	1,400 (1,100, 1,700)
500	0.00200	16 (13, 20)	1,800 (1,400, 2,300)
667	0.00150	18 (14, 24)	2,100 (1,600, 2,800)
1000	0.00100	22 (17, 30)	2,500 (2,000, 3,400)

FIGURE 9. Viral hemorrhagic fever exceedance probability function for Sub-Saharan Africa
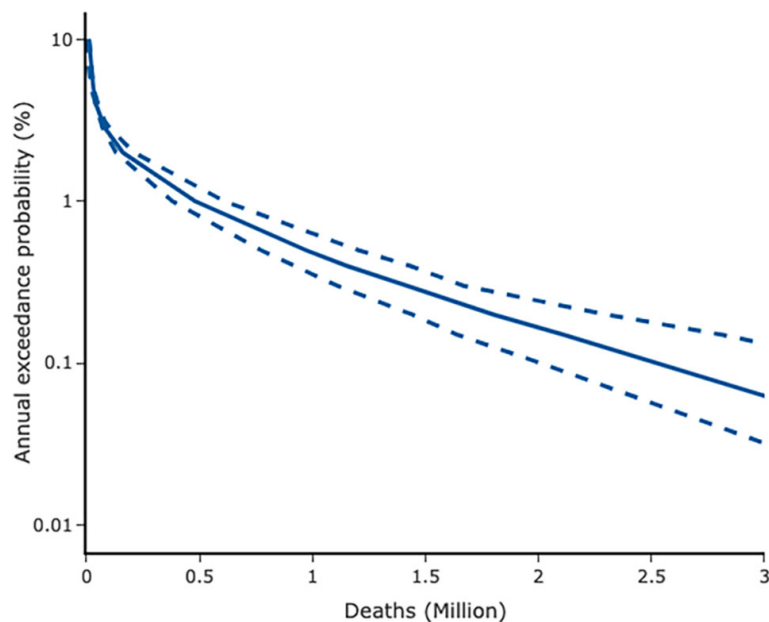
Our EPF estimates suggest that outbreaks such as the 2014 West Africa and the 2018 and 2021 Ebola virus disease epidemics in North Kivu are not aberrant events, but instead reflect the risk profile of the region. Our modeling framework produces simulated events on the scale and duration of these events, along with events that are much larger than what have been historically observed. Our model results suggest that larger VHF epidemics are more likely to occur than might be assumed if one derives risk estimates based on historical data alone (Box 2). Furthermore, the frequency and severity of VHF epidemics in Sub-Saharan Africa have increased in recent years (Stephens et al., 2022); if this trend continues, the risk of VHF events in Sub-Saharan Africa will increase even more over time.

As shown in Table 12, we estimate that a VHF epidemic causing approximately 10,000 deaths has an 8% annual probability of occurrence; viewed over a 10-year period, the risk of such an event occurring is roughly 57%. An event 5 times that magnitude, causing 50,000 deaths within Sub-Saharan Africa, has a roughly 3.7% annual probability. Such an event lies outside the range of historical experience, and appears improbable given the small annual probability; however viewed over a 10 year time period, it has a 31% probability of occurrence. Over a 25 year period, this increases to a 61% probability of occurrence.

TABLE 12. Annual, 5 year, 10 year, and 25 year exceedance probability (EP) estimates for selected Sub-Saharan Africa event sizes based on the VHF model event catalog

Deaths	Annual EP	5 Year EP	10 Year EP	25 Year EP
10,000	8.1%	34%	57%	88%
50,000	3.7%	17%	31%	61%
100,000	2.6%	12%	23%	48%

In the VHF model event catalog for Sub-Saharan Africa, total event sizes in death counts are smaller in magnitude than the respiratory catalog. Even so, about 2.5% of the events in the VHF model event catalog have at least 100,000 Sub-Saharan Africa regional deaths, while nearly 50% of all deaths in the catalog are from events having 1 million deaths or more in Sub-Saharan Africa (Figure 10).

FIGURE 10. VHF catalog composition: simulated event sizes and contribution to expected losses

Panel A: % of events

Panel B: % of deaths
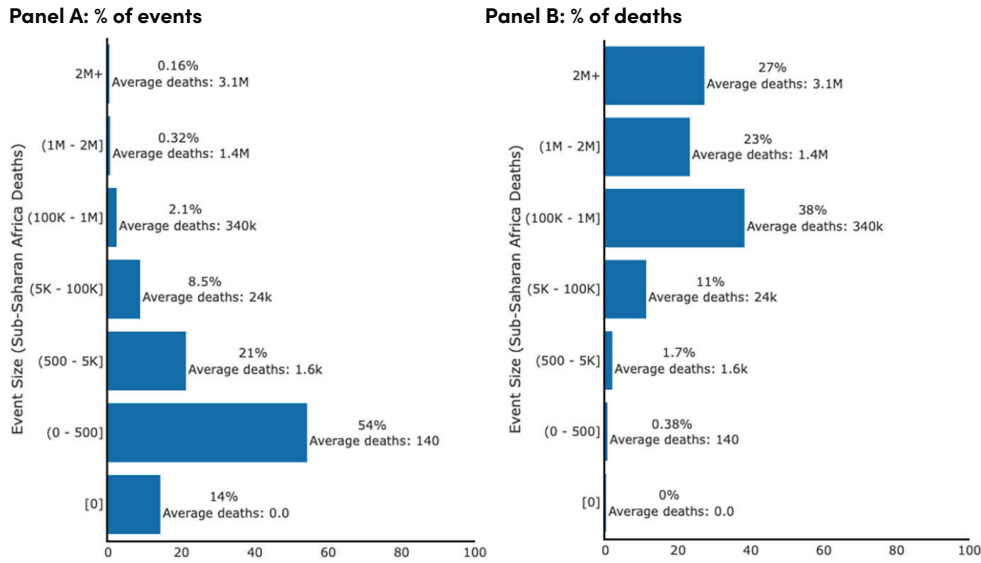
VHF mortality by age group

We calculated AAL for each of the modeled age groups. In contrast to the respiratory disease catalog, the normalized average annual deaths per 10,000 population varies considerably less across age groups. Figure 11 contains a graph of the normalized average annual deaths per 10,000 population for the VHF modeled event catalog in Sub-Saharan Africa. The graphed values are in Table 13. This analysis suggests that VHFs are more universally fatal, with mortality less differentiated by age than as seen with respiratory diseases (Garske et al., 2017; Rosello et al., 2015).

FIGURE 11. Average annual viral hemorrhagic fever deaths, by age group
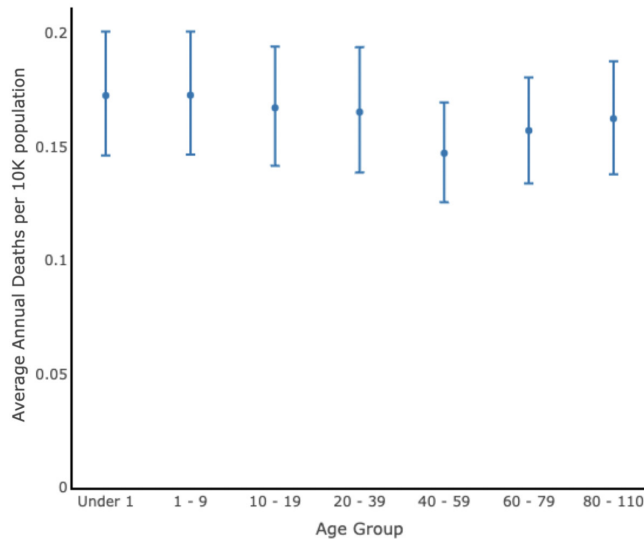
**TABLE 13. Sub-Saharan Africa average annual deaths
by age group based on VHF event catalog**

Age Group	Average Annual Deaths per 10,000 Population in that Age Group (95% Conf. Int)	Average Annual Deaths in that Age Group (Thousands) (95% Conf. Int)
Under 1	0.17	0.66
1–9	0.17	5.3
10–19	0.17	4.4
20–39	0.17	5.5
40–59	0.15	2.2
60–79	0.16	0.79
80–110	0.16	0.07
Sub-Saharan Africa Total	0.17	19

Discussion

Magnitude of epidemic & pandemic risk

The simulation-based results we present in this chapter demonstrate the scale of the risk posed by pathogens of epidemic potential. The estimated global average annual loss (AAL) of 2.5 million deaths represents a larger and more comprehensive accounting of the risk than was presented in DCP-3 (Fan et al., 2017; Madhav et al., 2017). The view of risk presented here—in particular the focus on losses in terms of deaths—also clearly represents a lower-bound estimate of total potential impact, since it does not include other sources of loss to human health and livelihoods (e.g., infections, hospitalizations, long-term sequelae, economic shocks, impacts on education, and societal disruption), nor—as we note above—does it include all sources of epidemic risk, such as vector-borne pathogens, bacterial infections, and viral threats presently unknown to science.

Our results also suggest that, among the diseases we modeled, respiratory diseases are the dominant driver of epidemic risk, with VHFs representing a relatively modest global risk in terms of expected deaths. VHFs are deadlier on an individual level, but less prone to spread than respiratory diseases. However, the risk is not negligible, especially in Sub-Saharan Africa, and merits attention based on the direct and indirect impacts of these events on lives and livelihoods (Sochas et al., 2017).

Effective priority setting in global health requires the comparison of disparate burdens and risks, some of which operate on different timescales. As such, it may be helpful to understand how our expected mortality estimates compare to other risks. It might seem intuitive to compare epidemic AAL to the annual mortality burden caused by endemic diseases, as these both represent average deaths per year. For example, the average annual deaths we estimate for respiratory epidemics is comparable in magnitude to the annual number of deaths caused by routinely-occurring endemic lower respiratory infections—approximately 2.4 million deaths (Troeger et al., 2018). However, when

comparing such estimates, it is important to keep in mind that the underlying patterns leading to these averages are very different. While the average annual deaths from endemic diseases is made up of moderate levels of loss that occur regularly, the epidemic AAL represents much larger spikes in losses that occur sporadically, punctuating stretches of non-epidemic years (Figure 1). Mortality spikes caused by low frequency, high severity events are potentially more economically disruptive than regularly-occurring endemic disease, suggesting that, even when AALs may be similar between both types of diseases, planning efforts towards high-impact epidemics should at least be equal to, if not greater than, endemic diseases.

Our model results also show that tail risk cannot be ignored. Low frequency, high severity events—the tail in our results—heavily drive expected deaths. It is all too easy to unconsciously discount the risk that the tail represents. The underrepresentation of extreme events in small sample sizes can lead policymakers to underweight their probability, especially when relying on a limited and biased historical dataset (Slovic & Weber, 2013). Moreover, the low annual probability of such extreme events tends to cause policy makers to round this probability down towards zero, due to cognitive biases that draw attention towards the frequency component of risk rather than the joint product of frequency *and* severity.

To compensate for this discounting bias, we have presented risk estimates for key points on the EPFs in terms of probability of occurrence over the next 5, 10 and 25 years. The results demonstrate how seemingly minute risks are far more substantial when viewed over a time horizon that is somewhat longer, but still relevant in terms of policy making and budgeting. Over a 10-year view, an event on the scale of COVID-19 has a roughly 25% probability of occurrence; over the next 25 years, such an event has a likelihood roughly equivalent to a coin toss. These estimates demonstrate that future epidemic risk is more substantial than commonly believed, and that severe events are likely to occur much more frequently than "once in a century" (Box 3).

Prevention, mitigation, and response strategies

The estimates that we present in this chapter do not, on their face, provide much cause for optimism. The expected losses from epidemic risk are enormous, and our results point to the considerable potential for pandemics that dwarf COVID-19 in terms of human impacts. But expectations can change. The risk estimates we presented are not immutable. Risk could increase if the global community does not take meaningful steps to address the underlying drivers of risk. Conversely, risk can be reduced through investments in prevention (e.g., spillover risk reduction), surveillance, preparedness, and response, which can be achieved through investments spanning basic necessities to technological innovations.

General investments in health system strengthening can significantly reduce epidemic losses, including those caused by respiratory diseases and VHFs. Because other important determinants outside of direct investment—such as technologies to produce medical countermeasures—may also

have changed over time, it is difficult to compare the benefits of improving preparedness between sporadic, severe crises. These investments can easily appear to be wasted on threats that do not materialize. Yet, investments to prepare for severe epidemics can also support effective responses to smaller events and other infectious disease risks, even in inter-pandemic periods. Such general investments having far-reaching benefits include, for example, improved laboratory capacity for rapid detection and confirmation of infectious disease threats (Wacharapluesadee et al., 2020), and border monitoring programs to track the importation risk of high-consequence pathogens (Wegrzyn et al., 2022). These improvements can also keep surveillance and response infrastructure "warm," that is, in continuous operational performance so it may persist in a constant state of readiness. Surveillance and response systems need to operate continuously, both between and during epidemics—so that they can be constantly utilized and stress-tested, and also so they can detect epidemics in the earliest days of their spark and emergence, since early action has the potential for greatest impact. Ultimately, building these capacities will provide the greatest opportunity to stop an outbreak before it becomes an epidemic, or globally catastrophic pandemic.

Localized outbreaks and smaller epidemics provide additional risk mitigation possibilities. For example, due to the more localized nature of VHFs, the spark location is more influential to the overall mortality for VHFs than for respiratory diseases (Madhav et al., 2020), and potential spark locations are good candidates for spillover reduction efforts. Additionally, for VHFs, interventions often are implemented with a more localized approach than respiratory diseases. For example, health officials have employed ring-vaccination, in contrast to mass vaccination, with *Zaire ebolavirus* vaccines and Marburg vaccine candidates (Cross et al., 2022). Furthermore, since localized epidemics are more geographically constrained, there is a greater likelihood for international cooperation because neighboring countries, and the international community, can spare more resources—such as workforce, supplies, and financial assistance—towards the affected country, and this can greatly improve outcomes.

Importance of a risk-informed lens

While it is impossible to predict the timing and magnitude of the next epidemic, risk modeling can provide informed views of the potential frequency and severity of future epidemics. The key question is: what exactly should the world be preparing for? Effectively preparing for an event as severe as the 1918 influenza pandemic could require very different strategies and levels of investment than would be needed, for example, to prepare for a COVID-19-level event. While it is infeasible and resource-inefficient to plan for every epidemic that could possibly occur, plans should be flexible and adaptable, to handle a wide range of possibilities. Careful consideration of the full range of potential epidemic scenarios can ensure that preparedness and response plans are commensurate with the level of risk, by guiding discussions about the types of surveillance and response systems that must be built, and the level of financing that is required. A risk-informed approach can help governments

make better decisions around preparedness, to ensure that the world is ready for the next pandemic while making efficient use of limited resources.

Decision makers traditionally have used a risk-informed analysis framework to prepare for other hazards besides epidemics. For example, in the design of wind loads for bridges, engineers often use a 2% annual probability (50-year return period) as a guideline (Garlich et al., 2015). Similarly, engineers may build urban road drainage systems to handle the flood risks from a precipitation event having a 2% annual probability (50-year return period), while they may build high-risk levees to withstand floods up to a 0.1% annual probability (1,000-year return period), due to the catastrophic consequences of failure (Ponce, 2008). Discussion of the suitability of these particular risk tolerance thresholds, and whether they should be adopted in planning for epidemic and pandemic risk, is important for risk-informed policymaking and effective resource allocation, but beyond the scope of this chapter. Further discussion may be found elsewhere (for example, see Strouth, et al., 2019).

Planners and decision makers can likewise develop risk-informed epidemic preparedness, mitigation, and response plans, relying on EPFs to provide necessary metrics. In practice, based on country resources and risk tolerance, decision makers would work towards a preparedness target for their country—for example, to be ready for an epidemic at a 5% annual probability (20 year return period). Being prepared to this level would imply that a country could effectively respond to an epidemic of that magnitude and bring it under containment. Countries could determine what their acceptable risk thresholds are for epidemics by using existing frameworks such as the Precautionary Principle or As Low As Reasonably Practicable (ALARP) (Pike et al., 2020).

To meet these risk thresholds, risk models can provide further details to help to design and calibrate specific investments. Risk modeling shows that transmissibility and case fatality ratio greatly influence overall epidemic severity for both respiratory pathogens and VHFs. Thus, the most impactful intervention measures for reducing mortality should target investments that reduce these factors. Towards this aim, risk modeling can be used to estimate stockpile sizes and resource needs for personal protective equipment, diagnostic tests, vaccine doses, antiviral drugs, and other therapeutics; as well as the effects of intervention timing; and the costs associated with implementing these measures. Risk models can also help countries to develop financing strategies, including risk transfer mechanisms, to offload portions of risk and response that are beyond their immediate budgetary capacity (Asian Development Bank, 2022; Madhav et al., 2020).

Larger epidemics require higher-level planning and may need to include provisions for regional cooperation to have the greatest chance at success. For example, developing regional vaccine manufacturing facilities may be a cost-effective and politically viable approach to building surge production capacity (Jha et al., 2021).

International standards for preparedness could also take a risk-informed approach, for example by setting benchmarks for risk tolerance and minimum preparedness levels to counter the potential

for a "weakest link" effect. Such a model could, for example, require that all countries be prepared to respond effectively to a respiratory event at the 5% annual probability level. This type of requirement could augment assessments such as the Joint External Evaluation (JEE), which sets standards for the prevention, preparedness and response systems capacities that countries must have in place, but does not specify what level of risk mitigation or reduction those capacities can achieve. Requiring that countries meet a common standard for risk tolerance and preparedness would also require sustained financing to meet and maintain the necessary capacities. For many low and middle-income countries, financing preparedness and response capacities is challenging, due to budgeting constraints and competing health system priorities, such as high-burden endemic diseases. However, early detection and mitigation of pathogens with epidemic and pandemic potential are a global public good, which protects the health, national security, and economic prosperity of all countries. Given the scale of the risk, the G20 High Level Independent Panel on Financing the Global Commons for Pandemic Preparedness and Response proposed a dramatic scale-up of financing, including substantial aid for low and middle income countries (Shanmugaratnam et al., 2021), which would allow these countries to meet minimum preparedness and response thresholds. One of the primary barriers to effective—and effectively-scaled—collective action is uncertainty regarding the magnitude and timing of future pandemics. This type of uncertainty has the well-characterized problem of leading to market failure (Arrow 1963)—in this case, underinvestment in global public goods such as surveillance and response capacities.

A risk-informed view can also prevent policymakers from falling victim to recency bias and over-calibrating to historical experience. For years, historical influenza pandemics were the planning benchmark for pandemic preparedness (US Department of Health and Human Services, 2005). The experience of the relatively mild 2009 influenza pandemic led some analysts to conclude that the global community had "overplanned" and overinvested (Low & McGeer, 2010). This may have even fueled the complacency and neglect that led to shortcomings in the global COVID-19 response. As the most recent severe pandemic, COVID-19 is likely to become a *de facto* planning benchmark. The modeling results we present here suggest that doing so would be short-sighted. Multiple pandemics have occurred over the past century, with varying characteristics and magnitudes. Extreme events modeling shows that a wider range of scenarios is possible and should be taken into consideration, to limit the risk of strategic surprise (Fukuyama, 2008). Furthermore, our model results suggest and historical experience corroborates that events more severe than previous historical observations can and do occur. The 2014 West Africa Ebola epidemic, which exceeded deaths during prior Ebola outbreaks by two orders of magnitude, vividly illustrates this point.

The results presented in this chapter strongly suggest that epidemic risk is far more persistent and substantial than is commonly believed. The probability exists that an epidemic—or even a large pandemic—could start in any year (Box 1). Our results demonstrate the urgency and priority of action to mitigate the risk. Armed with this knowledge, the world can be ready for the next major pandemic—which, in all likelihood, will not wait one hundred years to find us.

References

Arrow, K.J., (1963). Uncertainty and the welfare economics of medical care. The American Economic Review. *53*(5), 941–973.

Asian Development Bank. (2022). *Building Resilience to Future Outbreaks: Infectious Disease Risk Financing Solutions for the Central Asia Regional Economic Cooperation Regio.* http://dx.doi.org/10.22617/TCS220010-2.

Astengo, M., Tassinari, F., Paganino, C., Simonetti, S., Gallo, D., Amicizia, D., Piazza, M. F., Orsi, A., Icardi, G., & Ansaldi, F. (2021). Weight of risk factors for mortality and short-term mortality displacement during the COVID-19 pandemic. *Journal of Preventive Medicine and Hygiene*, *62*(4), E864.

Badker, R., Miller, K., Pardee, C., Oppenheim, B., Stephenson, N., Ash, B., Philippsen, T., Ngoon, C., Savage, P., Lam, C., & Madhav, N. (2021). Challenges in reported COVID-19 data: Best practices and recommendations for future epidemics. *BMJ Global Health*, *6*(5), e005542. https://doi.org/10.1136/bmjgh-2021-005542.

Baker, R. E., Mahmud, A. S., Miller, I. F., Rajeev, M., Rasambainarivo, F., Rice, B. L., Takahashi, S., Tatem, A. J., Wagner, C. E., Wang, L.-F., Wesolowski, A., & Metcalf, C. J. E. (2021). Infectious disease in an era of global change. *Nature Reviews Microbiology*. https://doi.org/10.1038/s41579-021-00639-z.

Bargain, O., & Aminjonov, U. (2020). Trust and compliance to public health policies in times of COVID-19. *Journal of Public Economics*, *192*, 104316.

Bennett, J. E., Dolin, R., & Blaser, M. J. (2019). *Mandell, douglas, and bennett's principles and practice of infectious diseases E-book.* Elsevier Health Sciences.

Carlson, C. J., Albery, G. F., Merow, C., Trisos, C. H., Zipfel, C. M., Eskew, E. A., Olival, K. J., Ross, N., & Bansal, S. (2022). Climate change increases cross-species viral transmission risk. *Nature*, *607*(7919), 555–562.

CDC. (2021). *What are VHFs?* https://www.cdc.gov/vhf/about.html.

Cherry, J. D. (2004). The chronology of the 2002–2003 SARS mini pandemic. *Paediatric Respiratory Reviews*, *5*(4), 262–269.

Cirillo, P., & Taleb, N. N. (2020). Tail risk of contagious diseases. *Nature Physics*, *16*(6), 606–613.

Contreras, S., Iftekhar, E. N., & Priesemann, V. (2023). From emergency response to long-term management: The many faces of the endemic state of COVID-19. *The Lancet Regional Health–Europe*.

Cross, R. W., Longini, I. M., Becker, S., Bok, K., Boucher, D., Carroll, M. W., Díaz, J. V., Dowling, W. E., Draghia-Akli, R., & Duworko, J. T. (2022). An introduction to the Marburg virus vaccine consortium, MARVAC. *PLoS Pathogens*, *18*(10), e1010805.

Cruickshank, M., & Shaban, R. Z. (2020). COVID-19: Lessons to be learnt from a once-in-a-century global pandemic. *Journal of Clinical Nursing*, *29*(21–22), 3901.

Diallo, M.S.K., Rabilloud, M., Ayouba, A., Touré, A., Thaurignac, G., Butel, C., Kpamou, C., Barry, T.A., Sall, M.D., Camara, I. & Leroy, S. (2019). Prevalence of infection among asymptomatic and paucisymptomatic contact persons exposed to Ebola virus in Guinea: A retrospective, cross-sectional observational study. *The Lancet Infectious Diseases*, *19*(3), 308–316.

Embrechts, P., Resnick, S. I., & Samorodnitsky, G. (1999). Extreme value theory as a risk management tool. *North American Actuarial Journal*, *3*(2), 30–41.

Fan, V. Y., Jamison, D., & Summers, L. H. (2017). The Loss from Pandemic Influenza Risk. In D. Jamison (Ed.), *Disease Control Priorities: Improving Health and Reducing Poverty* (world; 3rd ed., Vol. 9). World Bank.

Farzanegan, M. R., & Hofmann, H. P. (2022). A matter of trust? Political trust and the COVID-19 pandemic. *International Journal of Sociology*, *52*(6), 476–499.

FEMA. (2016). *The 100 Year Flood Myth*. https://training.fema.gov/hiedu/docs/hazrm/handout%203-5.pdf.

Fraser, C., Riley, S., Anderson, R. M., & Ferguson, N. M. (2004). Factors that make an infectious disease outbreak controllable. *Proceedings of the National Academy of Sciences of the United States of America*, *101*(16), 6146–6151. https://doi.org/10.1073/pnas.0307506101.

Fukuyama, F. (2008). *Blindside: How to anticipate forcing events and wild cards in global politics*. Rowman & Littlefield.

Garlich, M. J., Pechillo, T. H., Schneider, J. M., Helwig, T., O'Toole, M. A., Kaderbek, S.-L. C., Grubb, M. A., & Ashton, J. (2015). *Engineering for Structural Stability in Bridge Construction*. United States. Federal Highway Administration. Office of Bridge Technology.

Garske, T., Cori, A., Ariyarajah, A., Blake, I. M., Dorigatti, I., Eckmanns, T., Fraser, C., Hinsley, W., Jombart, T., Mills, H. L., Nedjati-Gilani, G., Newton, E., Nouvellet, P., Perkins, D., Riley, S., Schumacher, D., Shah, A., Kerkhove, M. D. V., Dye, C., … & Donnelly, C. A. (2017). Heterogeneities in the case fatality ratio in the West African Ebola outbreak 2013–2016. *Phil. Trans. R. Soc. B*, *372*(1721), 20160308. https://doi.org/10.1098/rstb.2016.0308.

Gates, B. (2020). Responding to Covid-19—A once-in-a-century pandemic? *New England Journal of Medicine*, *382*(18), 1677–1679.

Ginkgo Bioworks. (2023). *Spatiotemporal data for 2019-Novel Coronavirus Covid-19 Cases and deaths*. Humanitarian Data Exchange. https://data.humdata.org/dataset/2019-novel-coronavirus-cases.

Glennon, E. E., Jephcott, F. L., Restif, O., & Wood, J. L. N. (2019). Estimating undetected Ebola spillovers. *PLOS Neglected Tropical Diseases*, *13*(6), e0007428. https://doi.org/10.1371/journal.pntd.0007428.

Gomes, M. F. C., Pastore y Piontti, A., Rossi, L., Chao, D., Longini, I., Halloran, M. E., & Vespignani, A. (2014). Assessing the International Spreading Risk Associated with the 2014 West African Ebola Outbreak. *PLoS Currents*. https://doi.org/10.1371/currents.outbreaks. cd818f63d40e24aef769dda7df9e0da5.

Guterres, A. (2020). All hands on deck to fight a once-in-a-lifetime pandemic. *The United Nations COVID-19 Response.*

Han, B. A., Kramer, A. M., & Drake, J. M. (2016). Global Patterns of Zoonotic Disease in Mammals. *Trends in Parasitology*, *32*(7), 565–577. https://doi.org/10.1016/j.pt.2016.04.007.

Hoffman, B. L., & Fox, D. P. (2019). The 1918–1920 H1N1 Influenza A pandemic in Kansas and Missouri: Mortality patterns and evidence of harvesting. *Transactions of the Kansas Academy of Science*, *122*(3–4), 173–192.

Jamison, D. T., Summers, L. H., Alleyne, G., Arrow, K. J., Berkley, S., Binagwaho, A., … & Yamey, G. (2013). Global health 2035: A world converging within a generation. *The Lancet*, 382(9908), 1898–1955.

Jha, P., Jamison, D. T., Watkins, D. A., & Bell, J. (2021). A global compact to counter vaccine nationalism. *The Lancet*, *397*(10289), 2046–2047.

Johnson, N. P. A. S., & Mueller, J. (2002). Updating the Accounts: Global Mortality of the 1918–1920 "Spanish" Influenza Pandemic. *Bulletin of the History of Medicine*, *76*(1), 105–115. https://doi. org/10.1353/bhm.2002.0022.

Jones, B. A., Grace, D., Kock, R., Alonso, S., Rushton, J., Said, M. Y., McKeever, D., Mutua, F., Young, J., McDermott, J., & Pfeiffer, D. U. (2013). Zoonosis emergence linked to agricultural intensification and environmental change. *Proceedings of the National Academy of Sciences*, *110*(21), 8399–8404. https://doi.org/10.1073/pnas.1208059110.

Jones, K. E., Patel, N. G., Levy, M. A., Storeygard, A., Balk, D., Gittleman, J. L., & Daszak, P. (2008). Global trends in emerging infectious diseases. *Nature*, *451*(7181), 990–993. https://doi.org/ 10.1038/nature06536.

Kaplan, S., & Garrick, B. J. (1981). On the quantitative definition of risk. *Risk Analysis*, *1*(1), 11–27.

Kogan, N. E., Gantt, S., Swerdlow, D., Viboud, C., Semakula, M., Lipsitch, M., & Santillana, M. (2022). *Leveraging Serosurveillance and Postmortem Surveillance to Quantify the Impact of COVID-19 in Africa* (p. 2022.07.03.22277196). medRxiv. https://doi.org/10.1101/2022.07.03.22277196.

Kozlowski, R. T., & Mathewson, S. B. (1995). *Measuring and managing catastrophe risk*.

Ledesma, J. R., Isaac, C. R., Dowell, S. F., Blazes, D. L., Essix, G. V., Budeski, K., Bell, J., & Nuzzo, J. B. (2023). Evaluation of the Global Health Security Index as a predictor of COVID-19 excess mortality standardised for under-reporting and age structure. *BMJ Global Health*, *8*(7), e012203.

Lempert, R. J., & Light, P. C. (2009). Evaluating and implementing long-term decisions. *The RAND Frederick S. Pardee Center*, 11.

Low, D. E., & McGeer, A. (2010). Pandemic (H1N1) 2009: Assessing the response. *CMAJ*, *182*(17), 1874–1878.

Ma, J., Dushoff, J., & Earn, D. J. (2011). Age-specific mortality risk from pandemic influenza. *Journal of Theoretical Biology*, *288*, 29–34.

Madhav, N., Bosa, H. K., Agyarko, R. D., Stephenson, N., Miller, K., Gallivan, M., Lam, C., Meadows, A., Sridharan, V., & Bah, A. (2020). Development of a risk modeling approach to enhance the effectiveness of epidemic preparedness, response, and financing strategies in African countries. *International Journal of Infectious Diseases*, *101*, 212–213.

Madhav, N., Oppenheim, B., Gallivan, M., Mulembakani, P., Rubin, E., & Wolfe, N. (2017). Pandemics: Risks, Impacts, and Mitigation. In D. T. Jamison, H. Gelband, S. Horton, P. Jha, R. Laxminarayan, C. N. Mock, & R. Nugent (Eds.), *Disease Control Priorities: Improving Health and Reducing Poverty* (3rd ed.). The International Bank for Reconstruction and Development/The World Bank. http://www.ncbi.nlm.nih.gov/books/NBK525302/.

Madhav, N., Stephenson, N., & Oppenheim, B. (2021). *Multipathogen event catalogs—Technical note.* 24.

Marani, M., Katul, G. G., Pan, W. K., & Parolari, A. J. (2021). Intensity and frequency of extreme novel epidemics. *Proceedings of the National Academy of Sciences*, *118*(35), e2105482118. https://doi.org/10.1073/pnas.2105482118.

Meadows, A. J., Oppenheim, B., Guerrero, J., Ash, B., Badker, R., Lam, C. K., Pardee, C., Ngoon, C., Savage, P. T., & Sridharan, V. (2022). Infectious Disease Underreporting Is Predicted by Country-Level Preparedness, Politics, and Pathogen Severity. *Health Security*, *20*(4), 331–338.

Meadows, A. J., Stephenson, N., Madhav, N. K., & Oppenheim, B. (2023). Historical trends demonstrate a pattern of increasingly frequent and severe epidemics of high-consequence zoonotic viruses. *BMJ Global Health, 8*(11), p.e012026.

Meslé, M. M., Vivancos, R., Hall, I. M., Christley, R. M., Leach, S., & Read, J. M. (2022). Estimating the potential for global dissemination of pandemic pathogens using the global airline network and healthcare development indices. *Scientific Reports*, *12*(1), 3070.

Morens, D. M., Taubenberger, J. K., & Fauci, A. S. (2021). A centenary tale of two pandemics: The 1918 influenza pandemic and COVID-19, part I. *American Journal of Public Health*, *111*(6), 1086–1094.

Morens, D. M., Taubenberger, J. K., Folkers, G. K., & Fauci, A. S. (2010). Pandemic influenza's 500th anniversary. *Clinical Infectious Diseases*, *51*(12), 1442–1444.

Msemburi, W., Karlinsky, A., Knutson, V., Aleshin-Guendel, S., Chatterji, S., & Wakefield, J. (2023). The WHO estimates of excess mortality associated with the COVID-19 pandemic. *Nature*, *613*(7942), 130–137.

NCI. (2023). *Respiratory disease [definition]*. https://www.cancer.gov/publications/dictionaries/
cancer-terms/def/respiratory-disease.

Nelson, K. E., & Williams, C. M. (2014). *Infectious disease epidemiology: Theory and practice.*
Jones & Bartlett Publishers.

Olival, K. J., Hosseini, P. R., Zambrana-Torrelio, C., Ross, N., Bogich, T. L., & Daszak, P. (2017). Host
and viral traits predict zoonotic spillover from mammals. *Nature*, *546*(7660), 646–650.
https://doi.org/10.1038/nature22975.

Pike, H., Khan, F. & Amyotte, P. (2020). Precautionary principle (PP) versus as low as reasonably
practicable (ALARP): Which one to use and when. Process Safety and Environmental Protection,
137, 158–168.

Ponce, V. M. (2008). *Q & A on the return period to be used for design*. http://returnperiod.sdsu.edu/;
https://ponce.sdsu.edu/return_period.html.

Porta, M. (2014). *A dictionary of epidemiology*. Oxford university press.

Price-Smith, A. T. (2001). *The health of nations: Infectious disease, environmental change,
and their effects on national security and development*. MIT Press.

Resolve To Save Lives. (2021). *Epidemics that Didn't Happen*. https://preventepidemics.org/
epidemics-that-didnt-happen-2021/.

Rosello, A., Mossoko, M., Flasche, S., Hoek, A. J. V., Mbala, P., Camacho, A., Funk, S., Kucharski, A.,
Ilunga, B. K., Edmunds, W. J., Piot, P., Baguelin, M., & Tamfum, J.-J. M. (2015). Ebola virus disease
in the Democratic Republic of the Congo, 1976–2014. *ELife*, *4*, e09015. https://doi.org/10.7554/
eLife.09015.

Sands, P., Mundaca-Shah, C., & Dzau, V. J. (2016). The Neglected Dimension of Global Security—
A Framework for Countering Infectious-Disease Crises. *New England Journal of Medicine*,
374(13), 1281–1287. https://doi.org/10.1056/NEJMsr1600236.

Shanmugaratnam, T., Summers, L., Okonjo-Iweala, N., Botin, A., El-Erian, M., Frenkel, J., Grynspan,
R., Ishii, N., Kremer, M., & Mazumdar-Shaw, K. (2021). *A Global Deal for our Pandemic Age.*

Sirleaf, E. J., & Clark, H. (2021). Report of the Independent Panel for Pandemic Preparedness and
Response: Making COVID-19 the last pandemic. *The Lancet*, *398*(10295), 101–103.

Slovic, P., & Weber, E. U. (2013). Perception of risk posed by extreme events. *Regulation of Toxic
Substances and Hazardous Waste (2nd Edition)(Applegate, Gabba, Laitos, and Sachs, Editors),
Foundation Press, Forthcoming.*

Smith, K. F., Goldberg, M., Rosenthal, S., Carlson, L., Chen, J., Chen, C., & Ramachandran, S. (2014).
Global rise in human infectious disease outbreaks. *Journal of The Royal Society Interface*,
11(101), 20140950. https://doi.org/10.1098/rsif.2014.0950.

Sochas, L., Channon, A. A., & Nam, S. (2017). Counting indirect crisis-related deaths in the context of a low-resilience health system: The case of maternal and neonatal health during the Ebola epidemic in Sierra Leone. *Health Policy and Planning*, *32*(suppl_3), iii32–iii39.

Stephens, P. R., Sundaram, M., Ferreira, S., Gottdenker, N., Nipa, K. F., Schatz, A. M., Schmidt, J. P., & Drake, J. M. (2022). Drivers of African Filovirus (Ebola and Marburg) Outbreaks. *Vector-Borne and Zoonotic Diseases*, *22*(9), 478–490.

Strouth, A., McDougall, S., Jakob, M., Holm, K. & Moase, E. (2019). Quantitative risk management process for debris flows and debris floods: Lessons learned in Western Canada. Association of Environmental and Engineering Geologists; special publication 28.

Taubenberger, J. K., & Morens, D. M. (2006). 1918 Influenza: The Mother of All Pandemics. *Emerging Infectious Diseases*, *12*(1), 15–22. https://doi.org/10.3201/eid1201.050979.

Troeger, C., Blacker, B., Khalil, I. A., Rao, P. C., Cao, J., Zimsen, S. R., Albertson, S. B., Deshpande, A., Farag, T., & Abebe, Z. (2018). Estimates of the global, regional, and national morbidity, mortality, and aetiologies of lower respiratory infections in 195 countries, 1990–2016: A systematic analysis for the Global Burden of Disease Study 2016. *The Lancet Infectious Diseases*, *18*(11), 1191–1210.

United Nations Population Division. (2022). *World Population Prospects 2022: Data Sources. (UN DESA/POP/2022/DC/NO. 9)*. https://population.un.org/wpp/.

US Department of Health and Human Services. (2005). HHS pandemic influenza plan. *Washington (DC): The Department*.

van Wijhe, M., Ingholt, M. M., Andreasen, V., & Simonsen, L. (2018). Loose ends in the epidemiology of the 1918 pandemic: Explaining the extreme mortality risk in young adults. *American Journal of Epidemiology*, *187*(12), 2503–2510.

Vinck, P., Pham, P. N., Bindu, K. K., Bedford, J., & Nilles, E. J. (2019). Institutional trust and misinformation in the response to the 2018–19 Ebola outbreak in North Kivu, DR Congo: A population-based survey. *The Lancet Infectious Diseases*, *19*(5), 529–536.

Wacharapluesadee, S., Iamsirithawon, S., Chaifoo, W., Ponpinit, T., Ruchisrisarod, C., Sonpee, C., Katasrila, P., Yomrat, S., Ghai, S., & Sirivichayakul, S. (2020). Identification of a novel pathogen using family-wide PCR: Initial confirmation of COVID-19 in Thailand. *Frontiers in Public Health*, *8*, 598.

Wegrzyn, R. D., Appiah, G. D., Morfino, R., Milford, S. R., Walker, A. T., Ernst, E. T., Darrow, W. W., Li, S. L., Robison, K., & MacCannell, D. (2022). Early detection of SARS-CoV-2 variants using traveler-based genomic surveillance at four US airports, September 2021-January 2022. *MedRxiv*, 2022.03. 21.22272490.

WHO. (2020). COVID-19 Emergency Committee highlights need for response efforts over long term. *Geneva: WHO*, *1*, 2020.

WHO. (2022a). *Global excess deaths associated with COVID-19 (modelled estimates).* https://www.who.int/data/sets/global-excess-deaths-associated-with-covid-19-modelled-estimates.

WHO. (2022b). *WHO Coronavirus (COVID-19) Dashboard.* https://covid19.who.int.

Wilkinson, C. (2021). Pandemic data drives risk modeling. *Business Insurance.* https://www.businessinsurance.com/article/20210202/NEWS06/912339318/Pandemic-data-drives-risk-modeling-COVID-19-coronavirus-.

Wise, P. H., & Barry, M. (2017). Civil war & the global threat of pandemics. *Daedalus*, *146*(4), 71–84.

Annex A. Technical supplement

Supplemental material for:

Madhav, N. K., Oppenheim, B., Stephenson, N., Badker, R., Jamison, D. T., Lam, C., Meadows, A. J. Estimated Future Mortality from Pathogens of Epidemic & Pandemic Potential (2023). In: CGD Working Paper 665. Washington, DC: Center for Global Development.

Introduction

We developed an epidemic risk modeling framework to produce the estimates in this chapter. Our model draws upon principles from computational epidemiology, social science, economics, actuarial science, risk management, and extreme events modeling. It includes a disease spread model, development of exceedance probability curves, and estimation of the expected mortality. In this Technical Supplement, we provide detailed methods for each of these components.

Our disease spread model is a disease-specific, stochastic, global, metapopulation, compartmental model that simulates the daily spatio-temporal progression of disease spread. It includes mechanistic modeling of under-reporting to correct for uncertainty in reported infectious disease statistics and incorporates an Epidemic Preparedness Index (EPI) to model likely intervention scenarios and how they may differ for 200+ countries and territories (Oppenheim et al., 2019). Response measures are also included.

For each simulation within the event catalog, we derived plausible model input parameters and initial conditions from analyses of historical data and scientific literature. The simulations incorporate epidemiologic knowledge of pathogens and population characteristics that can impact transmission dynamics and the likelihood of severe outcomes.

In constructing the model, we included pandemic influenza and epidemic/novel coronaviruses to represent a catalog of epidemics and pandemics caused by respiratory pathogens having high pandemic potential. These included events caused by novel, human-to-human transmissible influenza A viruses and novel viruses in the subfamily Orthocoronavirinae that are zoonotic in origin and cause disease in humans, such as SARS-CoV-1, MERS-CoV, and SARS-CoV-2. Seasonal and endemic diseases, such as seasonal influenza and seasonal coronaviruses (which typically cause mild disease in humans), were considered to be part of the "baseline risk", which is adequately represented in historical mortality data, and were not included.

The output of our risk model is a modeled event catalog (Main Text, Table 1), which is a database containing many hypothetical views of the potential loss that may be experienced in a given year (Madhav et al., 2017, 2021). The event catalog serves as a basis for probabilistic estimation of potential human and economic losses caused by epidemics, and we used it to analyze the frequency and severity of infectious disease epidemics caused by respiratory pathogens of concern.

We generated the event catalogs using simulations produced by the disease spread model described above. Simulations are initiated with parameter values sampled from probability distributions. Parameters are instead held constant if they are relatively invariant across observed epidemics, are not influential to the model outcomes, or do not have sufficient historic data to develop a probability distribution. With our sampling approach the most probable parameter values are represented more often in the event catalog, and the extreme values for that parameter will rarely occur. The outcome of this process is an event catalog that captures the probabilities of the occurrence of different-magnitude events in any given year.

The frequency of events is a key driver of overall epidemic risk. The modeled event frequency is characterized either by the time between events in the historical record (i.e., inter-arrival time), or, for more frequently-occurring events, the number of epidemics per year. For pathogens that are rare, many simulated years in the event catalog do not contain any epidemic, while catalogs for more frequent events may contain more than one event per year.

Disease spread model

A key component of our risk modeling framework is a computational epidemiology-based disease spread model. The disease spread model begins with zoonotic disease spillover from an animal host and simulates human-to-human disease transmission between and within thousands of modeled geographic subpopulations across the world. The model framework consists of a stochastic, metapopulation compartment model coupled with human mobility networks overlaid across a human population layer, with underpinnings comparable to previously-published models (Balcan et al., 2009; Colizza et al., 2007), and including enhancements as described below.

Population layer

Our disease spread models operate over a global human population layer constructed from available census data and United Nations estimates (United Nations, 2015). Individuals are partitioned into subpopulations that correspond to administrative subdivisions. During simulations, individuals are assumed to interact homogeneously within each subpopulation. Disease is transmitted between and within each subpopulation on a daily time step.

Mobility model

Outbreaks spread locally within subpopulations as people interact with their communities, and across the globe through long-distance travel. In our disease spread model, pathogens spread between subpopulations through mobility networks. Long-range mobility (i.e., air travel) occurs on a daily time scale. Short-range mobility (i.e., daily commuting) occurs over a time period shorter than one day.

Global epidemic spread is facilitated by rapid human movement via airplanes. Air travel is incorporated into the disease spread model by probabilistically moving individuals between geographic subpopulations according to domestic and international air traffic data. Air traffic data, consisting of the number of individuals who travel between each airport, were used to calculate the daily probability of air travel between connected subpopulations (OAG, 2016). Each individual in an epidemiological model compartment that has the ability to travel (based on disease status) has the potential to move to a connected subpopulation every simulation day. This results in minor changes to the number of individuals in each subpopulation over time.

Our model also includes short-range mobility, which estimates the daily probability that an individual travels between two adjacent subpopulations. The short-range mobility model assumes that individuals that commute for work, in general, spend one-third of the day in their destination location and spend the remainder of the time in their origin location. This is a general assumption that reflects the average amount of time persons spend at work during a day. The proportion of the population that commutes each day is estimated at the country level based on the labor force, unemployment, and road networks.

Epidemic preparedness index

Epidemic preparedness and response capacity are important factors that influence outbreak severity. The Epidemic Preparedness Index (EPI) is a comprehensive metric used in the disease spread models to capture the geographic variation in outbreak preparedness and response capacity. The EPI reflects the geographic subpopulation's ability to detect and respond to an epidemic event, where scores range from 0 (least prepared) to 100 (most prepared) (Oppenheim et al., 2019).

Reporting bias

Real-world observational outbreak data are always affected by reporting biases because not all information is known or reported to health authorities, especially in real-time (Dalziel et al., 2018; Gamado et al., 2017). Reporting biases are notably present especially before the causative agent of the outbreak is known.

Our disease spread model output must be interpreted in light of reporting biases for comparison with real-world outbreak data. To address this issue, we built a model that estimates a pathogen-specific reporting rate at the national level. The estimated reporting rate from this model is used in the compartment model to more closely reflect the real number of cases. To develop this model, we collected pathogen- and country-specific reporting rates from the scientific literature along with potential predictor variables that can be used to inform the model (Meadows et al., 2022).

Epidemiological compartment model

To simulate disease spread, our epidemiologic model compartmentalizes human subpopulations by disease state. An individual can only exist in one disease state at any given time. The model probabilistically captures the progression of individuals through each disease state using a series of transition rates. Stochastic transitions between model compartments capture the inherent variation in disease transmission and progression. Compartment transitions are defined by discrete stochastic chain binomial and multinomial processes. The model calculates the number of individuals in each disease state by geographic subpopulation for each simulation day.

The epidemic model utilizes a specialized SEIHR (Susceptible–Exposed–Infectious–Hospitalized–Removed) compartmental structure shown in Figure A1. The ability to travel or commute and infect other individuals is defined for each compartment (Table A1). Infectious individuals can spread disease within their subpopulation and to other geographic subpopulations if the individuals travel. Mass vaccination campaigns are also explicitly incorporated into the compartment model structure.

FIGURE A1. Epidemiological compartment model
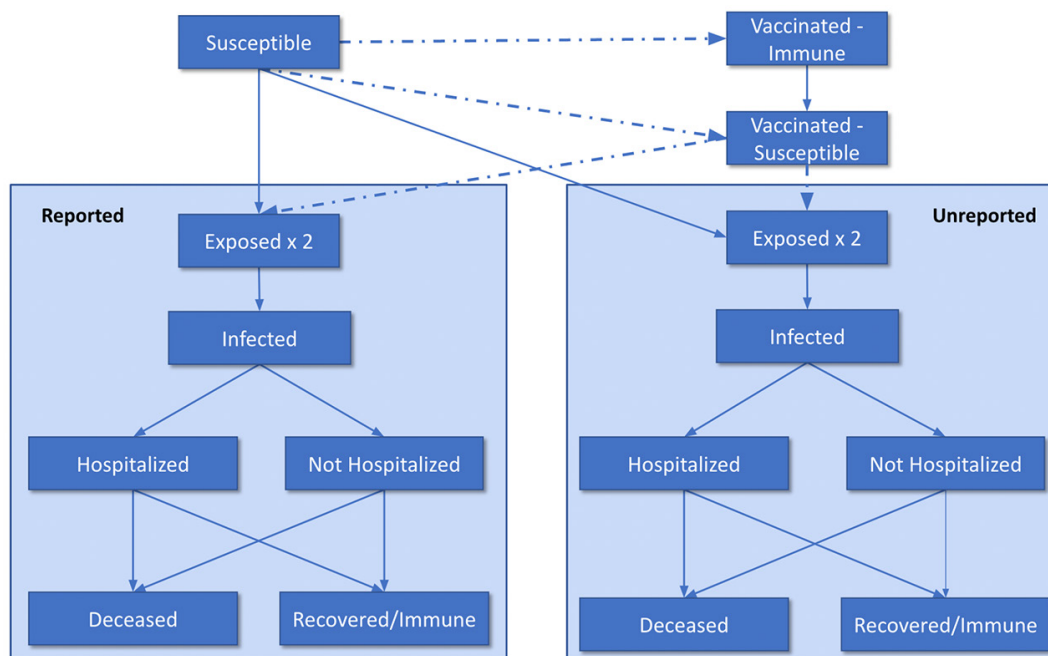
At the start of the event, all individuals are in the Susceptible compartment and a single individual is added to the Exposed compartment. The simulation continues until no individuals are in the Exposed, Infected, Hospitalized or Not-Hospitalized compartments. Long- and short-distance travel is explicitly modeled for Exposed and Infected compartments. Individuals in the Hospitalized,

Not-Hospitalized, and Deceased compartments are assumed to not travel. Air travel of Susceptible and Immune compartments is not modeled as they do not contribute to the movement of infection (Table A1).

TABLE A1. Description of modeled disease states, their infectivity, and ability to commute

State	Description	Mobility[†]	Infectious
Susceptible	Individuals susceptible to infection	Yes^	No
Exposed 1 and 2	Individuals exposed to disease, not yet infectious	Yes	No
Infected	Infected and showing symptoms	Yes	Yes
Not–Hospitalized	Infected individuals who are not treated in a traditional hospital setting	No	Yes
Hospitalized	Infected individuals who are hospitalized	No	Yes
Recovered	Individuals who have recovered from infection and are now immune	Yes^	No
Deceased	Individuals that have died of their infection and are not infectious	No	No
Vaccinated–Immune	Individuals who are vaccinated and become immune to future infection	No^	No
Vaccinated–Susceptible	Individuals who are vaccinated but do not achieve immunity and remain susceptible to future infection	No^	No

Notes: [†]Mobility indicates whether or not individuals in the state are incorporated into the long- and short-range mobility networks; ^Susceptible and Recovered individuals are only incorporated into short-range (not long-range) mobility networks due to computational constraints.

The modeled transition rate from the Susceptible to the Exposed state is determined by the Force of Infection. Exposed individuals progress through two sequential Exposed compartments so that the duration of the incubation period is Erlang-distributed. At this stage individuals are then assigned to Reported or Unreported status based on the reporting ratio. Then they progress into the Infected compartments at a daily rate, epsilon, the inverse of the average incubation period.

Individuals in the Infected compartments may then transition into the Hospitalized or Not-Hospitalized states at a daily rate, gamma. This rate is associated with the average time between symptom onset and healthcare utilization; however, the model also includes a Not-Hospitalized compartment that captures individuals not cared for in a traditional hospital setting. Individuals in these two compartments cannot travel. Individuals in the Hospitalized and Not-Hospitalized compartments then move into the Recovered, or Deceased state at a daily rate, mu, based on the average time to recovery or death and case fatality ratio. Transition rates are shown in Table A2.

TABLE A2. Description of model transition rates

Transition	Transition Rates
Susceptible → Exposed 1	FOI
Exposed 1 → Exposed 2–Reported	epsilon/2 * RR
Exposed 1 → Exposed 2–Unreported	epsilon/2 * (1–RR)
Exposed 2 → Infected	(epsilon/2)
Infected → Hospitalized	gamma * CHR
Infected → Not-Hospitalized	gamma * (1–CHR)
Hospitalized/Not-Hospitalized → Recovered/Immune	mu * (1–CFR)
Hospitalized/Not-Hospitalized → Deceased	mu * CFR
Susceptible → Vaccinated–Immune^	VxRate * VxEff
Susceptible → Vaccinated–Susceptible^	VxRate * (1–VxEff)

Notes: CHR = Case hospitalization ratio; CFR = Case fatality ratio; FOI = Force of infections; RR = reporting ratio; VxRate = Vaccination Rate; VxEff = Vaccination Efficacy; ^Transitions from the Susceptible compartment to the Vaccinated-Immune and Vaccinated-Susceptible compartments only occur after the Vaccination Start Day and continue until the maximum proportion of the population to be vaccinated is achieved.

The force of infection (FOI; Eqn. A1) dictates the rate of transition from Susceptible to Exposed and is based on the reproduction number (R_t), the infectious period ($gamma^{-1}$), the total number of infectious individuals in the subpopulation, and the total number of individuals in the subpopulation (N_i). FOI is calculated for each subpopulation, i, on each day, t, using the equation:

$$FOI_{i,t} = \frac{R_t}{\left(\dfrac{1}{gamma}\right)} * \frac{(Total\ Infectious)_i}{N_i} \tag{A1}$$

Model parameterization

Model parameter distributions are estimated through review and analysis of the scientific literature and historical data, including from prior events and modeling studies (Table A3). The fitted distributions may be parametric or non-parametric, discrete or continuous, as warranted by the data and biological plausibility. The process of distribution fitting and assessment is shown in Figure A2.

Model parameters have varying levels of available data from historical events and the scientific literature that would allow for fitting of statistical distributions. There may be several reasons why parameters are less well-represented in the historical record and scientific literature, including a lack of historical events, lack of published data, or a lack of interest from the scientific community in estimating a particular parameter.

FIGURE A2. Process for fitting model parameter distributions
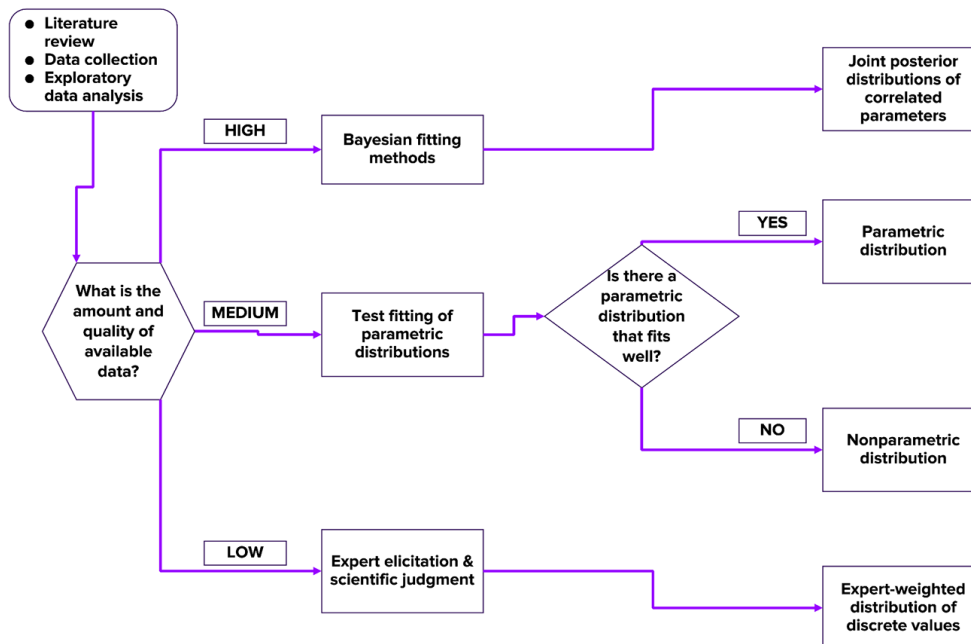
TABLE A3. Model parameter types and ranges of values (and references)

Parameter	Pandemic Influenza	MERS–Like Coronaviruses	SARS–Like Coronaviruses
R_0 (basic reproduction number)	Non–parametric (min = 1.0, max = 3.0) (Balcan et al., 2009; Jackson et al., 2010; Longini et al., 2005; Rizzo et al., 2011; Tuite et al., 2010; White et al., 2009; White & Pagano, 2008; Yang et al., 2009; Zhang Shenghai et al., 2009)	Triangular (min = 0.5, max = 0.9) (Breban et al., 2013; Cauchemez et al., 2014)	Triangular (min = 0.5, max = 2.8) (Adam et al., 2020; Chowell et al., 2015; Lipsitch et al., 2003)
K (superspreading dispersion parameter)	None	Uniform (min = 0.05, max = 0.10) (Choe et al., 2020)	Uniform (min = 0.35, max = 0.45) (Adam et al., 2020; Lau et al., 2020)
Incubation period (days)	Non–parametric (min = 1, max = 4) (Lessler et al., 2009; World Health Organization, 2009)	Truncated Lognormal (min = 1, max = 14) (Cauchemez et al., 2014)	Gamma (min = 1, max = 6) (Alene et al., 2021; McAloon et al., 2020)
Infectious period	Lognormal (min = 2, max = 5) (Carrat et al., 2008; Longini et al., 2005; Rvachev & Longini, 1985; Tizzoni et al., 2012; Tuite et al., 2010)	Fixed value (value = 5.2) (Cauchemez et al., 2014)	Fixed value (value = 5.2) (Cauchemez et al., 2014)

Transmissibility, whose initial value in the model is represented by R_0, is influenced by pathogen characteristics, host characteristics, and population/environmental characteristics, including population density, social interaction, and sanitation practices. The R_0 parameter is well-characterized in the scientific literature for several pathogens, due to the strong scientific and public health interest in understanding the transmissibility of pathogens. Infectious period is also well-represented in the scientific literature, albeit not as represented as R_0. This is because most methodologies for estimating infectious periods require clinical observations or viral shedding studies, while R_0 can be estimated solely from case counts over time, which are more likely to be publicly reported.

Intervention and response measures

Epidemic preparedness and response are critical determinants of event trajectory. The complexities of outbreak preparedness and response are captured in the disease spread model through a series of intervention parameters that capture activities that result in the reduction in the disease transmission rate, such as infection control improvements and social distancing. Model parameters pertaining to interventions are highlighted in Table A4, with distributions and ranges shown in Table A5.

Epidemic response strategies typically include pharmaceutical and non-pharmaceutical interventions. Pharmaceutical interventions can reduce transmission by preventing infection or reducing pathogen shedding; alternatively, pharmaceutical interventions may reduce the case fatality ratio by improving patients' clinical course. Examples of pharmaceutical interventions include vaccines and therapeutics. Non-pharmaceutical interventions encompass efforts to reduce transmission, such as improved sanitation, social distancing, and reduced population mobility. Examples include masking, contact tracing, quarantine, isolation, or "lockdowns", as occurred during COVID-19, and can also include mitigation of risks associated with cultural factors that play a role in transmission. Non-pharmaceutical interventions also include basic patient supportive care. The effectiveness of interventions depends heavily on social and political factors, such as the willingness of the public to comply with health regulations and adopt risk-reducing behavior. Therefore, effective risk communication and building population trust are critical aspects of epidemic response.

Epidemic control measures can include quarantine, isolation, strict infection control procedures in healthcare settings, antiviral therapies, and vaccination. Factors that determine the impacts of these control measures include time to deployment, available resources, and the ability to effectively communicate with the affected communities (Liu et al., 2015).

Due to the infrequency of large scale epidemics, there is a lack of information about how countries will respond. Additionally, these responses have changed significantly in the last few decades,

making information from historic events less reliable. For example, during the forty years spanning 1980–2020 there was only one influenza pandemic that tested the public health system's ability to detect a novel influenza virus and create and distribute a new vaccine. For this reason, such parameters have greater uncertainty and rely to a greater extent on the elicitation of expert opinion and scientific judgment.

TABLE A4. Model parameters associated with interventions and vaccination

Parameter	Description
Vaccination Rate	Proportion of the susceptible population that is vaccinated per day
Vaccine Efficacy	If a vaccine is available, the proportion of vaccinated individuals who become immune to infection
Vaccine Proportion	If a vaccine is available, the maximum proportion of the population that is vaccinated
Vaccine Deployment Time	If a vaccine is available, the time between the start of the event and vaccine deployment.
Intervention Time	The time between the start of the event and attempt at outbreak containment.
Intervention R_t	The effective reproduction number after intervention

Vaccination campaigns

For respiratory pathogen outbreaks, mass vaccine campaigns are explicitly modeled using model parameters as described in Tables A4–A5. The probability of vaccination (when a vaccine is available) is dependent upon these parameters.

The Vaccine Efficacy parameter indicates the proportion of vaccinated individuals who experience complete protection from the modeled virus infection (Nichol & Treanor, 2006). Vaccine Efficacy is set to zero if vaccination resources are not available during the modeled scenario, although other nonpharmaceutical interventions, which reduce transmission, still occur. This represents the possibility of resource limitations preventing vaccination campaigns.

The number of vaccines available during an outbreak is represented by the Vaccine Proportion variable. The parameter is intended to reflect the potential challenges in production and provision of vaccinations as well as vaccine uptake by the population. Vaccine Proportion is applied in the model by tracking the number of doses administered. Once the Vaccine Proportion is reached, Vaccination Rate is set to 0.

The Vaccine Deployment Time varies by simulation. Prior to the Vaccine Deployment Time, the Vaccination Rate for all subpopulations is zero. Once Vaccine Deployment Time occurs, members of each subpopulation receive vaccine on a daily basis, according to Vaccination Rate parameter, which varies by EPI.

General intervention measures

In addition to vaccination campaigns, the model includes an overall reduction in transmissibility due to non-pharmaceutical intervention (NPI) response measures, which represents an attempt at containment. In the model, transmissibility after implementation of the intervention measures is described by the parameter, R_t (the effective reproduction number at time t) (Bo et al., 2021).

The Intervention Time parameter describes when transmission reduction starts to occur as a result of intervention measures. Due to the limited historical data on time to intervention, we used the time difference between the onset of the first case to the time of first report as a proxy measure for intervention time. Reporting timeliness has been used as a proxy measure in previous research to assess surveillance and response systems (Chan et al., 2010).

The preparedness and response capacity of a region, based on EPI, is assumed to impact the Intervention Time parameter. Intervention Time is represented by a negative binomial distribution for each subpopulation according to their EPI equal interval quantile category. The negative binomial distribution was derived by fitting the distribution to the number of days between the onset of the first case (as reported in any data source) and the date of first report by the World Health Organization Disease Outbreak News reports (Oppenheim et al., 2019). This analysis contains data from January 1996 through August 2018, and excludes events caused by toxin, chemical, foodborne, vector-borne, or unknown pathogens. The empirical distribution of time to report by EPI quantile is displayed in Figure A3.

FIGURE A3. Time to report by Epidemic Preparedness Index (EPI) equal interval quantile
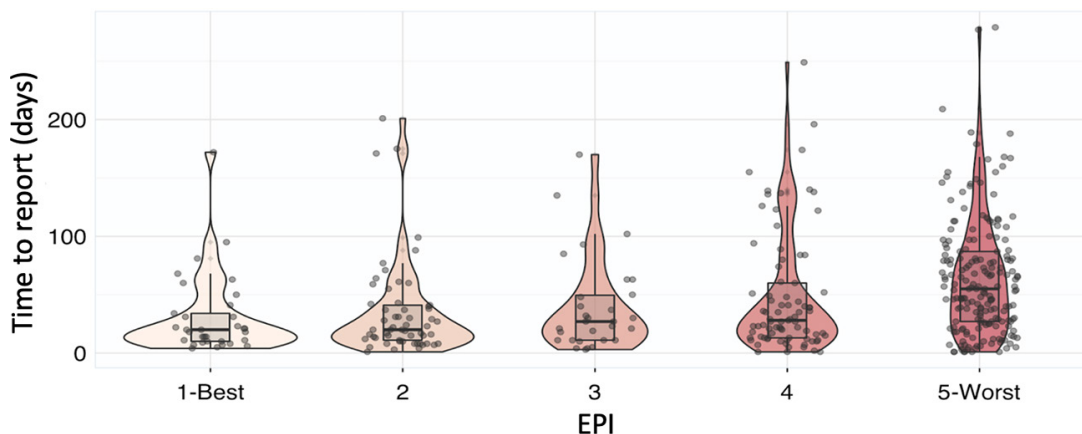
The value of R_t after interventions is based on the estimated efficacy of non-pharmaceutical response measures. Once a simulated event reaches the Intervention Time, the modeled transmissibility parameter is decreased linearly over the following two-week time period until R_t equals the new value. The R_t values are assumed based on observations from previous epidemics and modeling studies (Bo et al., 2021; Wu et al., 2006).

Outcomes modeling

Hospitalizations are modeled based on the Case Hospitalization Ratio (CHR) distribution, estimated by analysis from scientific literature and available data. The CHR estimates the proportion of infections that become ill enough to require and obtain hospital care.

Mortality is modeled based on the Case Fatality Ratio (CFR) distribution, which is also estimated based on analysis of scientific literature and available data. The CFR represents the proportion of infections that succumb to the illness.

There is strong evidence of correlation between the CHR and CFR, which is incorporated in the model (Figure A4). The assumed distributions of CHR and CFR are shown in Table A5.

FIGURE A4. Modeled relationship between case fatality ratio (CFR) and case hospitalization ratio (CHR)
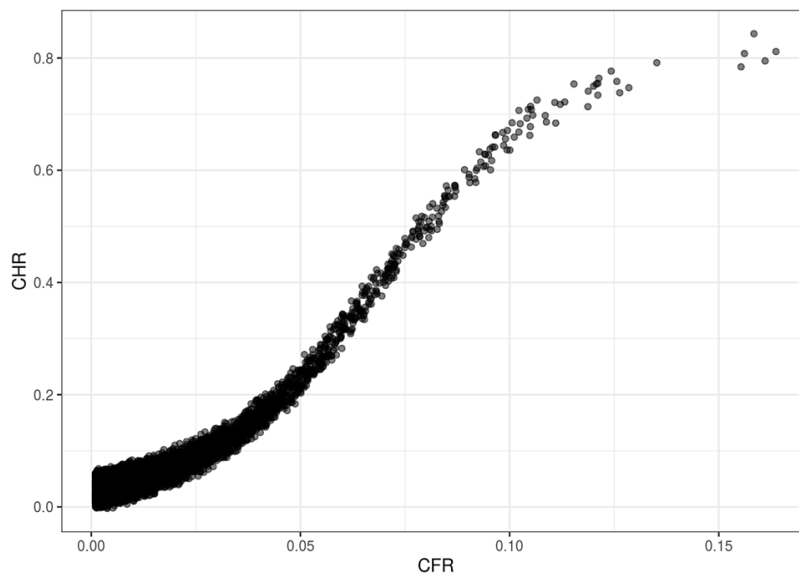
TABLE A5. Intervention and outcome parameter distributions and ranges (and references)

Parameter	Pandemic Influenza	MERS-Like Coronaviruses	SARS-Like Coronaviruses
CHR	Non-parametric (min= 0.0004, max = 0.4) (Andreasen et al., 2008; Chowell et al., 2011; Gani et al., 2005; Presanis et al., 2009; Shrestha et al., 2011; Shubin et al., 2014; Wu et al., 2010)	Triangular (min = 0.95, max = 1) (Rivers et al., 2016)	Function of CFR (Angulo et al., 2021)
CFR	Non-parametric (min = 0.00017, max = 0.29) Varies by EPI quintile (Britten, 1932; Lee et al., 2008; Valleron et al., 2010; Wong et al., 2013)	Triangular (min = 0.3, max = 0.4) (Majumder et al., 2014; Rambaut, Andrew, n.d.; Rivers et al., 2016)	Beta (min = 0, max = 0.24) (Grewelle & Leo, 2020; Jia et al., 2009; Kenyon, 2020; Liang et al., 2007; Luo et al., 2021; World Health Organization, 2015)
Vaccination Rate (Proportion of population per day)	Uniform (min = 0.045%, max = 1.1%) (Henderson et al., 2009; Mihigo et al., 2012; Tizzoni et al., 2012; World Health Organization, 2013)	None (Tai et al., 2022)	Gamma (min = 0%, max = 4.2%) Varies by EPI quintile (Richie et al., 2021)
Vaccine Efficacy	Discrete (min = 0.60, max = 0.80) (Longini et al., 2004)	None (Tai et al., 2022)	Uniform (min = 0.5, max = 0.8) (Cochrane Emergency and Critical Care Group et al., 2023)
Vaccine Proportion	Based on CHR, varies by country (Mihigo et al., 2012; Tizzoni et al., 2012; World Health Organization, 2013)	None (Tai et al., 2022)	Uniform (min = 0.5, max = 0.8) (Richie et al., 2021)
Vaccine Deployment Time (Start Day)	Discrete (min = 180, max = ∞) Varies by EPI quintile (Hessel & European Vaccine Manufacturers (EVM) Influenza Working Group, 2009; World Health Organization, 2013)	None (Tai et al., 2022)	Uniform (min = 120, max = 600) Varies by EPI quintile (Richie et al., 2021)
Intervention Time (weeks)	Discrete (min = 4, max = 12) (Martinez & Das, 2014; Oppenheim et al., 2019)	Fixed value (value = 52) Based on (Breban et al., 2013)	Uniform (min = 10, max = 32) (Ali et al., 2020)
Intervention R_t	R_0 reduction (min = 3%, max = 10%) Varies by EPI quintile (Martinez & Das, 2014; Oppenheim et al., 2019)	Fixed value (value = 0.5) Based on (Breban et al., 2013)	Decay over time (Ali et al., 2020; Chowell et al., 2004) Analysis of (Ginkgo Bioworks, 2023)

Spark location

The location at which a zoonotic infectious disease emerges into human populations can impact the extent and severity of an epidemic. Respiratory epidemics can start anywhere in the world, but several factors can increase the risk of an area becoming a spark site. The likely location of epidemic emergence ("spark location") is modeled through geospatial analysis of environmental variables, animal host locations, socioeconomic factors, and observed outbreak data. These data are formulated into emergence risk maps to identify high risk areas. This method often reveals areas of risk where cases have never been historically reported. The analyses performed are comparable to published works related to emergence mapping (Messina et al., 2016), such as for avian influenza and coronavirus spillover risk (Anthony et al., 2017; Dhingra et al., 2016; Sikkema et al., 2019).

Spark probabilities by country were estimated separately for pandemic influenza, MERS-like coronaviruses, and SARS-like coronaviruses (Tables A6–A8); estimates were aggregated up to regional groupings of countries. For all three categories, Asia and Africa had the greatest spark risk. For MERS-like coronaviruses, over 90% of the risk was concentrated in Asia, largely driven by high probabilities in the Middle East.

TABLE A6. Proportion of spark risk by region for pandemic influenza viruses

Region	Probability
Asia	33.53%
Africa	18.36%
North America	17.20%
South America	13.09%
Europe	11.60%
Oceania	6.22%

TABLE A7. Proportion of spark risk by region for MERS-like coronaviruses

Region	Probability
Asia	92.92%
Africa	5.42%
Oceania	0.96%
South America	0.32%
North America	0.21%
Europe	0.17%

TABLE A8. Proportion of spark risk by region for SARS-like coronaviruses

Region	Probability
Asia	31.66%
Africa	26.36%
North America	14.71%
Europe	13.78%
South America	10.27%
Oceania	3.21%

Event frequency

Distributions of event frequency were developed from an analysis of historical data. Some types of events, such as MERS-like coronaviruses, typically have multiple occurrences per year, while less frequent events, such as pandemic influenza and SARS-like coronaviruses, would have, on average, less than one event per year (Table A9).

TABLE A9. Parameterization of event frequency by pathogen category (and references)

Pathogen Category	Frequency Distribution
Pandemic Influenza (inter-arrival time, years)	Weibull (min = 5, max = 135) (Morens et al., 2010)
MERS-like Coronaviruses (events per year)	Truncated Negative Binomial (min = 15, max = 26) (Eifan et al., 2017)
SARS-like Coronaviruses (events per year)	Poisson (min = 0, max = 4) Analysis of (Ginkgo Bioworks, 2022)

Event catalog construction

For the results presented in this chapter, we simulated 100,000 years, representing 100,000 versions of "next year". The catalog size is determined by the number of simulations needed to achieve convergence in the tail risk estimates. Once the full set of stochastic simulations completes, it typically includes hundreds of thousands to millions of event scenarios, which are then compiled into an event catalog (Madhav et al., 2021).

For each modeled event catalog, we create two versions. The first version is the Total Direct Catalog, which includes a full view of all spillover events and total case and death counts, not just those that are detected and reported. This catalog view allows for a more complete accounting of the true picture of loss. The second version is the Reported Catalog, which is adjusted for both the probability of detecting an event and the ratio at which cases and deaths are reported. This catalog version better reflects the realities of epidemic reporting and is more readily comparable to historical reported data. In keeping with the framework presented in the main text section on "Direct Deaths vs. Excess Mortality", the estimates in the Reported Catalog represent Category D alone, while the Total Direct Catalog represents the sum of Categories C and D.

Exceedance probability functions

Once we create an event catalog, we use it to develop a discretized exceedance probability function (EPF). This function results in estimates for the probability that an event of severity, *s,* or greater will occur in a given year. The EPF encapsulates two key factors, the frequency and severity of epidemics, into one function. For this study, we used deaths as the severity metric, though other measures of severity could be used (e.g., cases, economic losses, etc.). Specifically, we used the annualized EPF. Annualization is achieved as such: if there are multiple epidemics in a simulated year, losses are aggregated by the year in which they start.

Operationally, the EPF is generated by sorting observation years in descending order and dividing the rank number by the total number of years in the event catalog. The simulated, discrete EPF is defined mathematically in the following way. Let S be a set of N independent severity observations having the members $\{S_1, S_2, S_3, ..., S_N\}$, where each S_j is the aggregation of losses beginning in each time period *j*. When the members of S are arranged in descending order, that is, the maximum S_j is first and the minimum S_j is last (in this example $(S_3 >= S_1 >= S_N >= ... >= S_2)$, and R_j is the rank number of the S_j observation (in this example, $R_3 = 1$, $R_1 = 2$, $R_N = 3$, ..., $R_2 = N$), then the exceedance probability function of S_j is estimated as shown in Equation A2.

$$EPF(S_j) = \frac{R_j}{(N+1)}$$
(A2)

An example EPF plot is provided in Figure A5.

FIGURE A5. Example exceedance probability function

s (severity, for example in deaths)
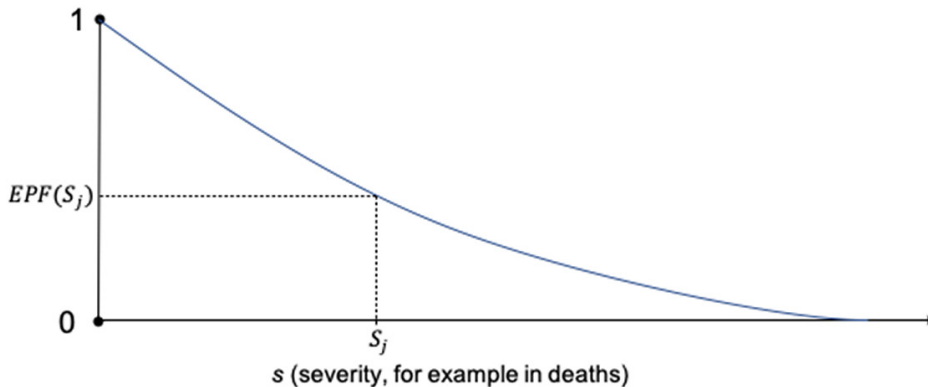
The inverse of EPF(*s*), *r*, is the return time (also known as return period or recurrence interval), shown in Equation A3.

$$r(s) = \frac{1}{EPF(s)}$$
(A3)

Some simulation years may have an equal number of deaths. To account for this, Equation A4 gives the formulation of the discrete probability density function (pdf) associated with the EPF, where N is the number of simulation years and n(s) is the number of simulation years resulting in severity s.

$$pdf(s) = \{\frac{n(s)}{N} \quad \text{if } s \geq 0, 0 \quad \text{if } s < 0. \tag{A4}$$

By probability theory, in the general case, the cumulative distribution function, $cdf(s)$ is defined by Equation A5

$$cdf(s) = \int_{-\infty}^{s} pdf(x)dx \tag{A5}$$

The EPF is simply the complementary cumulative distribution function, as shown in Equation A6.

$$EPF(s) = 1 - cdf(s) \tag{A6}$$

Expected value calculation

A summary statistic of the EPF is the expected value (EV) of severity in a year, where we use the term expected value as it is used in probability theory. In extreme events modeling and insurance, this is known as the average annual loss (AAL). The AAL for an infectious disease event catalog is the mean number of cases, hospitalizations, deaths, or associated monetary loss across all simulation years in the event catalog. The value is highly skewed due to the inclusion of extreme events in the catalog. Additionally, for rare events, there are many years within the EPFs with low levels of deaths, punctuated by some years with very high numbers of deaths. The expected severity value of the discrete EPFs, is given by Equation A7.

$$EV(EPF) = \sum_{s} s \cdot pdf(s) \tag{A7}$$

In the continuous treatment, the expected value of the number of deaths for a given EPF is the area under the EPF curve, given by Equation A8.

$$EV(EPF) = \int_{0}^{\infty} EPF(s)ds \tag{A8}$$

Model validation & sensitivity testing

Scenario inspection

We inspected a subset of scenarios to assess for biological and epidemiological plausibility. Below we provide examples of two different hypothetical scenarios simulated by our disease spread model (Table A10). These events illustrate what potential scenarios might look like and are just two of thousands of example scenarios within the catalogs. The event magnitudes of 12 million and 80 million total global deaths (Table A11) were selected based on falling in different portions of the respiratory pathogen EPF. Events of this magnitude can take many forms, given the myriad of model parameters and the stochastic nature of the simulations. Notably, in both of these scenarios, the epidemic simmers at low levels of transmission before taking off and becoming a global pandemic (Figure A6).

TABLE A10. Scenario input parameters

Parameter	Scenario 1	Scenario 2
Spark Country	Canada	Turkey
Incubation period (days)	3	5
R_0	1.679	1.716
Case-Fatality Ratio	1.74%	4.54%
Case-Hospitalization Ratio	6.64%	13.55%
Detection threshold	5 deaths	25 deaths
Timing of non-pharmaceutical interventions (NPIs)	30 days after detection in the spark country and 60 days after detection elsewhere	30 days after detection in the spark country and 60 days after detection elsewhere
R_t after interventions	0.9934	1.0502
Vaccination Rate (Proportion of population per day)	0.22% Varies by EPI	0.22% Varies by EPI
Vaccine Efficacy	0.8	0.8
Vaccine Proportion	0.7 Varies by EPI	0.7 Varies by EPI
Vaccine Development Time	326 days after detection Varies by EPI	326 days after detection Varies by EPI

TABLE A11. Estimated scenario outcomes

Outcome	Scenario 1	Scenario 2
Infection Counts (thousands)	686,000	1,800,000
Hospitalization Counts (thousands)	47,000	249,000
Death Counts (thousands)	12,300	83,300

FIGURE A6. Simulated epidemic curves for scenario 1: 12 million global deaths and scenario 2: 80 million global deaths
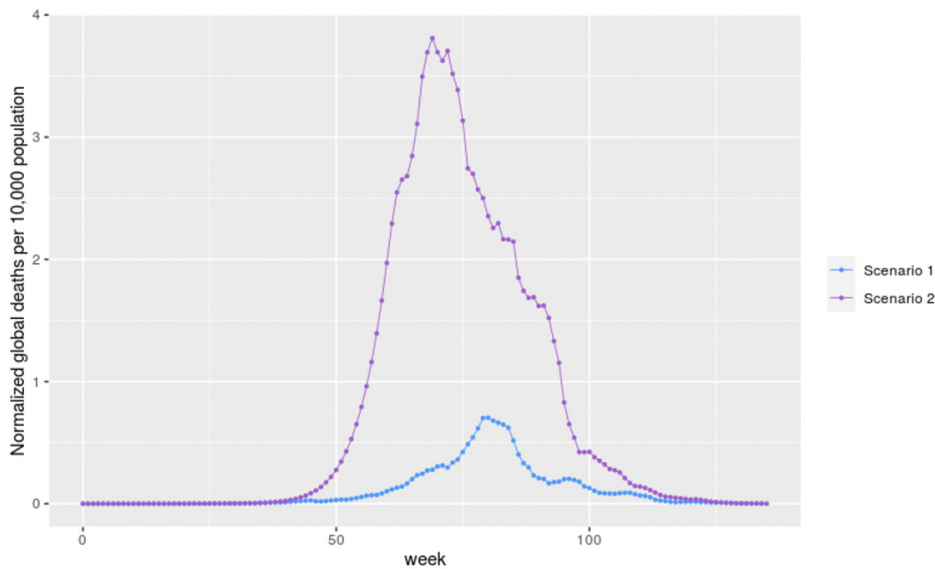
Sensitivity testing

We performed sensitivity analyses on our model to determine the response of the model to variations in parameter values. We analyzed the total number of infections as the output of interest. The analysis first required the simulation of a set of baseline scenarios. Then, additional simulations were produced by varying a single parameter around the baseline value while keeping all other parameters constant. This process was repeated for each model parameter. The list of parameters tested can be found in Table A12.

A sensitivity index based on partial rank correlation coefficients was calculated for each parameter and displayed in a tornado plot (Table A12, Figure A7). Sensitivity indices for vaccine-related, and non-vaccine parameters were run separately as a non-vaccine baseline scenario was used to test non-vaccine related parameters.

Based on the sensitivity analysis, we found that intervention timing, vaccine timing, and R_0 are strongly influential parameters in the overall simulated outbreak size. Incubation period is moderately influential, and the remaining parameters are only mildly influential. These findings are consistent with what is expected based on manual inspection of model output, basic epidemiological principles, and what is found in the literature for similar models.

TABLE A12. Sensitivity testing results demonstrated by partial rank correlation coefficients

Parameter	Original	Bias	Std. Error	Min. c.i.	Max. c.i.
R_0	0.4053	0.0020	0.0342	0.3376	0.4729
Intervention Time	0.0018	−0.0002	0.0397	−0.0806	0.0785
Incubation Period	−0.0866	0.0002	0.0397	−0.1637	−0.0107
Intervention R_t	0.1794	0.0005	0.0391	0.1048	0.2525
Vaccine Efficacy	0.0572	−0.0012	0.0393	−0.0139	0.1393
Vaccine Start Day	−0.0492	0.0002	0.0408	−0.1280	0.0316
Vaccine Proportion	0.0264	−0.0010	0.0407	−0.0513	0.1059

FIGURE A7. Graphical depiction of sensitivity testing results
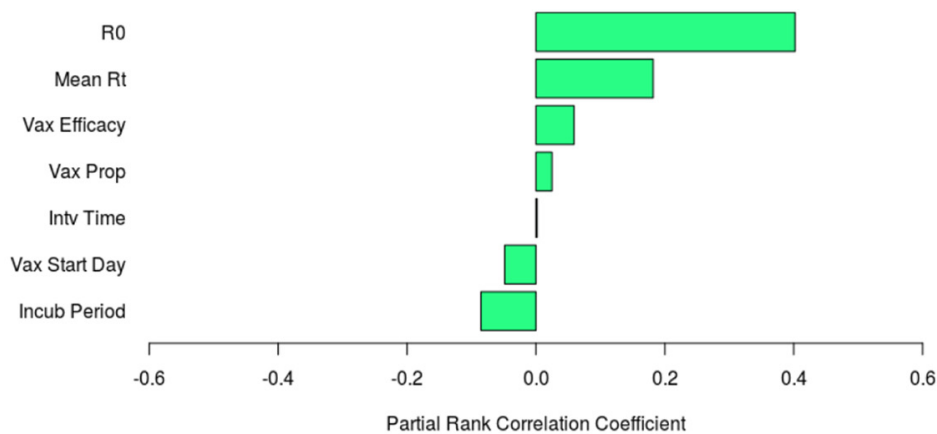
Historical event comparison

We conducted testing of the disease spread model to assess for concordance of model results with historical events. We simulated pandemics using parameter values similar to those reported in the scientific literature for historical events, including prior influenza and coronavirus pandemics. Here we discuss the validation efforts for the 2009 influenza pandemic and COVID-19. These two events occurred in a world that bears a closer resemblance to the world we model and the inherent assumptions (e.g., population structure, mobility patterns, medical countermeasures) are more applicable than for earlier pandemics.

For the 2009 influenza pandemic, we compared mortality estimates to historical estimates found in the scientific literature (Dawood et al., 2012). Results are shown in Figure A8. Given the probabilistic nature of confidence intervals, it is expected that some model estimates would fall outside of the ranges recorded, and this was found to be the case particularly for lower income countries like Afghanistan. This may be due to incomplete surveillance of influenza-related mortality in those locations.

FIGURE A8. Model comparison of influenza-related deaths to historical estimates for the 2009 influenza pandemic in select countries. Historical estimates from (Dawood et al., 2012)
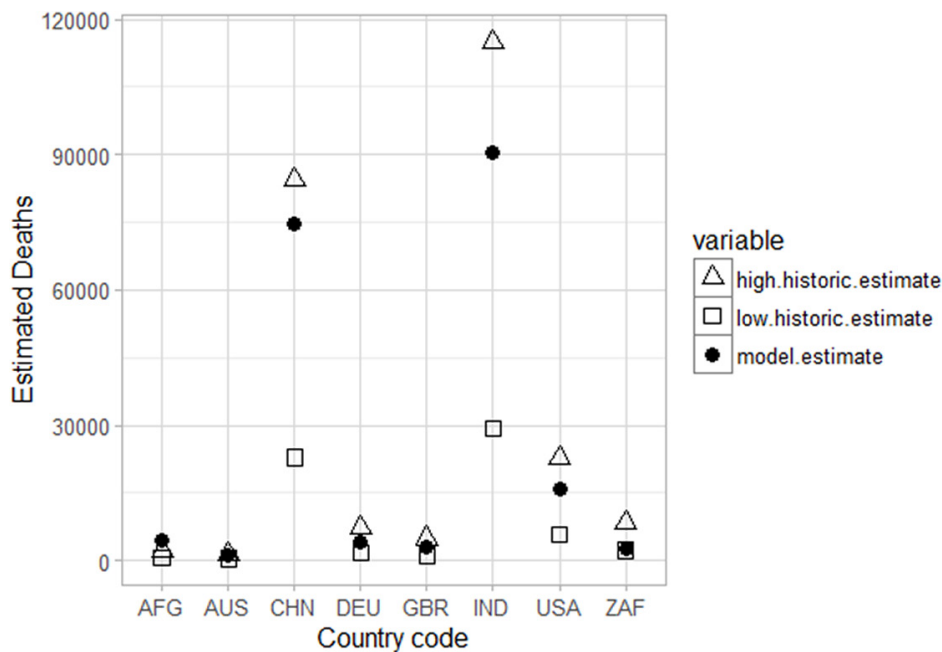
To assess the temporal progression of the 2009-like pandemic simulation, we compared the timing of the peak incidence to historical event data (Archer et al., 2009; Centers for Disease Control and Prevention, 2010; Choudhry et al., 2012; Echevarría-Zuno et al., 2009; Infectious Disease Surveillance Center (Japan), 2012; Merler et al., 2011; Oliveira et al., 2009; Tizzoni et al., 2012). In this comparison, we found that the timing of the modeled peak incidence for the 2009 pandemic showed good agreement to historical data (Figure A9). During this simulation, most countries experienced their highest number of symptomatic cases within a few weeks of historic estimates. This suggests the human mobility network and disease transmission processes within the model portray rates of disease spread in a realistic fashion. The slight delay from the model could result from assumptions on the spark timing of the event, transmissibility reduction due to seasonality, or temporal biases in case ascertainment.

FIGURE A9. Week of peak symptomatic cases, 2009 influenza pandemic
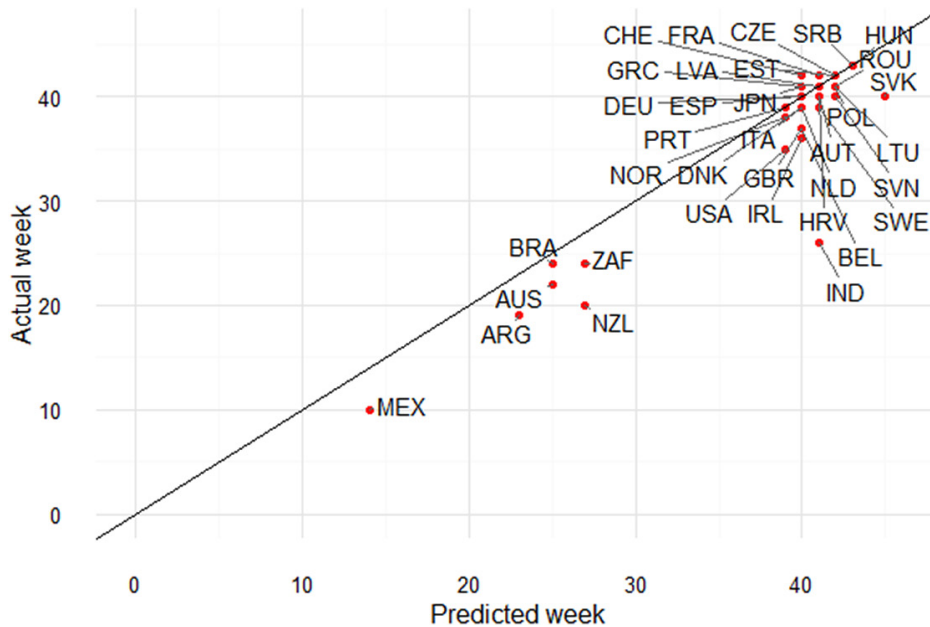
Results from a model fitting and comparison exercise we performed for the COVID-19 pandemic is reported elsewhere (Oppenheim et al., n.d.; United Nations, 2021). This comparison showed reasonable agreement of event trajectory and magnitude of estimates between modeled and historical data.

Historical benchmarking

Policymakers and planners also tend to benchmark modeled losses against historical experience. We therefore estimated the exceedance probabilities (EPs) of historical events based on our modeled EPF, to estimate these events' contemporary probability of occurrence (Table A13). To perform this analysis, we obtained reported mortality data from notable historical epidemics, estimated the proportion of the global population these deaths represented at the time of the event, and then calculated the number of deaths that the same proportion would represent for the 2020 global population (United Nations, Department of Economic and Social Affairs, Population Division, 2022). The mortality estimate for each event was then used in conjunction with our EPF to estimate the EP value and extrapolated to the 10-year cumulative EP (CEP) based on the formula provided in the main text.

For historical benchmarking, unlike most of the estimates presented elsewhere in this chapter and supplementary materials, we used our modeled Reported Catalog, rather than the Total Direct Catalog. We take this approach for historical benchmarking because historically reported information is more directly comparable to the Reported Catalog rather than the Total Direct Catalog.

TABLE A13. Estimated exceedance probabilities (EPs) for notable historical respiratory epidemics & pandemics

Event (Years)	Global Reported Deaths (Thousands) (Madhav et al., 2017)	Global Reported Deaths, Adjusted to 2020 Population (Thousands)	Global Reported Deaths (% mortality)	Annual EP	10-Year EP
SARS (2003)	0.774	0.944	0.00001%	8–9%	57–61%
COVID-19 (2019–2022)	6,500	6,500	0.08%	2–3%	18–26%
1957 Influenza Pandemic (1957–1958)	700–1,500	1,872–3,978	0.02%–0.05%	3.5–5.0%	30–40%
1968 Influenza Pandemic (1968–1970)	1,000	2,184	0.03%	4.4–4.8%	36–39%
2009 Influenza Pandemic (2009–2010)	152–576	156–624	0.002%–0.01%	6–7%	46–52%
1918 Influenza Pandemic (1918–1920)	20,000–100,000	86,580–432,900	1.11%–5.55%	<0.001%	<1%

Annex A references

Adam, D. C., Wu, P., Wong, J. Y., Lau, E. H. Y., Tsang, T. K., Cauchemez, S., Leung, G. M., & Cowling, B. J. (2020). Clustering and superspreading potential of SARS-CoV-2 infections in Hong Kong. *Nature Medicine*, 1–6. https://doi.org/10.1038/s41591-020-1092-0.

Alene, M., Yismaw, L., Assemie, M. A., Ketema, D. B., Gietaneh, W., & Birhan, T. Y. (2021). Serial interval and incubation period of COVID-19: A systematic review and meta-analysis. *BMC Infectious Diseases*, *21*, 1–9.

Ali, S. T., Wang, L., Lau, E. H. Y., Xu, X.-K., Du, Z., Wu, Y., Leung, G. M., & Cowling, B. J. (2020). Serial interval of SARS-CoV-2 was shortened over time by nonpharmaceutical interventions. *Science*, eabc9004. https://doi.org/10.1126/science.abc9004.

Andreasen, V., Viboud, C., & Simonsen, L. (2008). Epidemiologic Characterization of the 1918 Influenza Pandemic Summer Wave in Copenhagen: Implications for Pandemic Control Strategies. *The Journal of Infectious Diseases*, *197*(2), 270–278. https://doi.org/10.1086/524065.

Angulo, F. J., Finelli, L., & Swerdlow, D. L. (2021). Estimation of US SARS-CoV-2 infections, symptomatic infections, hospitalizations, and deaths using seroprevalence surveys. *JAMA Network Open*, *4*(1), e2033706–e2033706.

Anthony, S. J., Johnson, C. K., Greig, D. J., Kramer, S., Che, X., Wells, H., Hicks, A. L., Joly, D. O., Wolfe, N. D., & Daszak, P. (2017). Global patterns in coronavirus diversity. *Virus Evolution*, *3*(1), vex012.

Archer, B. N., Cohen, C., Naidoo, D., Thomas, J., Makunga, C., Blumberg, L., Venter, M., Timothy, G. A., Puren, A., & McAnerney, J. M. (2009). Interim report on pandemic H1N1 influenza virus infections in South Africa, April to October 2009: Epidemiology and factors associated with fatal cases. *Eurosurveillance*, *14*(42), 19369.

Balcan, D., Colizza, V., Gonçalves, B., Hu, H., Ramasco, J. J., & Vespignani, A. (2009). Multiscale mobility networks and the spatial spreading of infectious diseases. *Proceedings of the National Academy of Sciences, USA*, *106*(51), 21484–21489.

Bo, Y., Guo, C., Lin, C., Zeng, Y., Li, H. B., Zhang, Y., Hossain, M. S., Chan, J. W., Yeung, D. W., & Kwok, K. O. (2021). Effectiveness of non-pharmaceutical interventions on COVID-19 transmission in 190 countries from 23 January to 13 April 2020. *International Journal of Infectious Diseases*, *102*, 247–253.

Breban, R., Riou, J., & Fontanet, A. (2013). Interhuman transmissibility of Middle East respiratory syndrome coronavirus: Estimation of pandemic risk. *The Lancet*, *382*(9893), 694–699. https://doi.org/10.1016/S0140-6736(13)61492-0.

Britten, R. H. (1932). The Incidence of pandemic Influenza, 1918-19: A Further Analysis According to Age, Sex, and Color of the Records of Morbidity and Mortality Obtained in Surveys of 12 Localities. *Public Health Reports*, *47*(6), 303–375.

Carrat, F., Vergu, E., Ferguson, N. M., Lemaitre, M., Cauchemez, S., Leach, S., & Valleron, A.-J. (2008). Time Lines of Infection and Disease in Human Influenza: A Review of Volunteer Challenge Studies. *American Journal of Epidemiology*, *167*(7), 775–785. https://doi.org/10.1093/aje/kwm375.

Cauchemez, S., Fraser, C., Van Kerkhove, M. D., Donnelly, C. A., Riley, S., Rambaut, A., Enouf, V., van der Werf, S., & Ferguson, N. M. (2014). Middle East respiratory syndrome coronavirus: Quantification of the extent of the epidemic, surveillance biases, and transmissibility. *The Lancet Infectious Diseases*, *14*(1), 50–56. https://doi.org/10.1016/S1473-3099(13)70304-9.

Centers for Disease Control and Prevention. (2010). Update: Influenza activity-United States, 2009-10 season. *MMWR. Morbidity and Mortality Weekly Report*, *59*(29), 901–908.

Chan, E. H., Brewer, T. F., Madoff, L. C., Pollack, M. P., Sonricker, A. L., Keller, M., Freifeld, C. C., Blench, M., Mawudeku, A., & Brownstein, J. S. (2010). Global capacity for emerging infectious disease detection. *Proceedings of the National Academy of Sciences of the United States of America*, *107*(50), 21701–21706. https://doi.org/10.1073/pnas.1006219107.

Choe, S., Kim, H.-S., & Lee, S. (2020). Exploration of Superspreading Events in 2015 MERS-CoV Outbreak in Korea by Branching Process Models. *International Journal of Environmental Research and Public Health*, *17*(17), Article 17. https://doi.org/10.3390/ijerph17176137.

Choudhry, A., Singh, S., Khare, S., Rai, A., Rawat, D. S., Aggarwal, R. K., & Chauhan, L. S. (2012). Emergence of pandemic 2009 influenza A H1N1, India. *The Indian Journal of Medical Research*, *135*(4), 534.

Chowell, G., Abdirizak, F., Lee, S., Lee, J., Jung, E., Nishiura, H., & Viboud, C. (2015). Transmission characteristics of MERS and SARS in the healthcare setting: A comparative study. *BMC Medicine*, *13*(1), 210.

Chowell, G., Castillo-Chavez, C., Fenimore, P. W., Kribs-Zaleta, C. M., Arriola, L., & Hyman, J. M. (2004). Model Parameters and Outbreak Control for SARS. *Emerging Infectious Diseases*, *10*(7), 1258–1263. https://doi.org/10.3201/eid1007.030647.

Chowell, G., Echevarría-Zuno, S., Viboud, C., Simonsen, L., Tamerius, J., Miller, M. A., & Borja-Aburto, V. H. (2011). Characterizing the Epidemiology of the 2009 Influenza A/H1N1 Pandemic in Mexico. *PLOS Medicine*, *8*(5), e1000436. https://doi.org/10.1371/journal.pmed.1000436.

Cochrane Emergency and Critical Care Group, Graña, C., Ghosn, L., Evrenoglou, T., Jarde, A., Minozzi, S., Bergman, H., Buckley, B. S., Probyn, K., & Villanueva, G. (2023). Efficacy and safety of COVID-19 vaccines. *Cochrane Database of Systematic Reviews*, *2023*(3).

Colizza, V., Barrat, A., Barthelemy, M., Valleron, A.-J., & Vespignani, A. (2007). Modeling the worldwide spread of pandemic influenza: Baseline case and containment interventions. *PLoS Medicine*, *4*(1), e13.

Dalziel, B. D., Lau, M. S. Y., Tiffany, A., McClelland, A., Zelner, J., Bliss, J. R., & Grenfell, B. T. (2018). Unreported cases in the 2014-2016 Ebola epidemic: Spatiotemporal variation, and implications for estimating transmission. *PLOS Neglected Tropical Diseases*, *12*(1), e0006161. https://doi.org/10.1371/journal.pntd.0006161.

Dawood, F. S., Iuliano, A. D., Reed, C., Meltzer, M. I., Shay, D. K., Cheng, P.-Y., Bandaranayake, D., Breiman, R. F., Brooks, W. A., Buchy, P., Feikin, D. R., Fowler, K. B., Gordon, A., Hien, N. T., Horby, P., Huang, Q. S., Katz, M. A., Krishnan, A., Lal, R., … & Widdowson, M.-A. (2012). Estimated global mortality associated with the first 12 months of 2009 pandemic influenza A H1N1 virus circulation: A modelling study. *The Lancet Infectious Diseases*, *12*(9), 687–695. https://doi.org/10.1016/S1473-3099(12)70121-4.

Dhingra, M. S., Artois, J., Robinson, T. P., Linard, C., Chaiban, C., Xenarios, I., Engler, R., Liechti, R., Kuznetsov, D., Xiao, X., Dobschuetz, S. V., Claes, F., Newman, S. H., Dauphin, G., & Gilbert, M. (2016). Global mapping of highly pathogenic avian influenza H5N1 and H5Nx clade 2.3.4.4 viruses with spatial cross-validation. *ELife*, *5*. https://doi.org/10.7554/eLife.19571.

Echevarría-Zuno, S., Mejía-Aranguré, J. M., Mar-Obeso, A. J., Grajales-Muñiz, C., Robles-Pérez, E., González-León, M., Ortega-Alvarez, M. C., Gonzalez-Bonilla, C., Rascón-Pacheco, R. A., & Borja-Aburto, V. H. (2009). Infection and death from influenza A H1N1 virus in Mexico: A retrospective analysis. *The Lancet*, *374*(9707), 2072–2079.

Eifan, S. A., Nour, I., Hanif, A., Zamzam, A. M. M., & AlJohani, S. M. (2017). A pandemic risk assessment of middle east respiratory syndrome coronavirus (MERS-CoV) in Saudi Arabia. *Saudi Journal of Biological Sciences*, *24*(7), 1631–1638. https://doi.org/10.1016/j.sjbs.2017.06.001.

Gamado, K., Streftaris, G., & Zachary, S. (2017). Estimation of under-reporting in epidemics using approximations. *Journal of Mathematical Biology*, *74*(7), 1683–1707. https://doi.org/10.1007/s00285-016-1064-7.

Gani, R., Hughes, H., Fleming, D., Griffin, T., Medlock, J., & Leach, S. (2005). Potential Impact of Antiviral Drug Use during Influenza Pandemic. *Emerging Infectious Diseases*, *11*(9), 1355–1362. https://doi.org/10.3201/eid1109.041344.

Ginkgo Bioworks. (2022). *Global Epidemic Monitoring and Modeling Platform [Data Source]*. https://gemm.solutions.concentricbyginkgo.com/.

Ginkgo Bioworks. (2023). *Spatiotemporal data for 2019-Novel Coronavirus Covid-19 Cases and deaths*. Humanitarian Data Exchange. https://data.humdata.org/dataset/2019-novel-coronavirus-cases.

Grewelle, R. E., & Leo, G. A. D. (2020). *Estimating the Global Infection Fatality Rate of COVID-19* (p. 2020.05.11.20098780). https://doi.org/10.1101/2020.05.11.20098780.

Henderson, D. A., Courtney, B., Inglesby, T. V., Toner, E., & Nuzzo, J. B. (2009). Public health and medical responses to the 1957-58 influenza pandemic. *Biosecurity and Bioterrorism: Biodefense Strategy, Practice, and Science*, *7*(3), 265–273.

Hessel, L. & European Vaccine Manufacturers (EVM) Influenza Working Group. (2009). Pandemic influenza vaccines: Meeting the supply, distribution and deployment challenges. *Influenza and Other Respiratory Viruses*, *3*(4), 165–170.

Infectious Disease Surveillance Center (Japan). (2012). *Influenza cases reported per sentinel weekly, 2002-2012*. http://idsc.nih.go.jp/idwr/kanja/weeklygraph/01flu-e.html.

Jackson, C., Vynnycky, E., & Mangtani, P. (2010). Estimates of the Transmissibility of the 1968 (Hong Kong) Influenza Pandemic: Evidence of Increased Transmissibility Between Successive Waves. *American Journal of Epidemiology*, *171*(4), 465–478. https://doi.org/10.1093/aje/kwp394.

Jia, N., Feng, D., Fang, L., Richardus, J. H., Han, X., Cao, W., & De Vlas, S. J. (2009). Case fatality of SARS in mainland China and associated risk factors. *Tropical Medicine & International Health*, *14*(s1), 21–27.

Kenyon, C. (2020). COVID-19 Infection Fatality Rate Associated with Incidence—A Population-Level Analysis of 19 Spanish Autonomous Communities. *Biology*, *9*(6), Article 6. https://doi.org/10.3390/biology9060128.

Lau, M. S. Y., Grenfell, B., Thomas, M., Bryan, M., Nelson, K., & Lopman, B. (2020). Characterizing superspreading events and age-specific infectiousness of SARS-CoV-2 transmission in Georgia, USA. *Proceedings of the National Academy of Sciences*, *117*(36), 22430–22435. https://doi.org/10.1073/pnas.2011802117.

Lee, V. J., Wong, C. S., Tambyah, P. A., Cutter, J., Chen, M. I., & Goh, K. T. (2008). Twentieth century influenza pandemics in Singapore. *ANNALS-ACADEMY OF MEDICINE SINGAPORE*, *37*(6), 470.

Lessler, J., Reich, N. G., Brookmeyer, R., Perl, T. M., Nelson, K. E., & Cummings, D. A. (2009). The Incubation Periods of Acute Respiratory Viral. *Lancet Infectious Diseases*, *9*, 291–300.

Liang, W., McLaws, M.-L., Liu, M., Mi, J., & Chan, D. K. Y. (2007). Hindsight: A re-analysis of the severe acute respiratory syndrome outbreak in Beijing. *Public Health*, *121*(10), 725–733. https://doi.org/10.1016/j.puhe.2007.02.023.

Lipsitch, M., Cohen, T., Cooper, B., Robins, J. M., Ma, S., James, L., Gopalakrishna, G., Chew, S. K., Tan, C. C., & Samore, M. H. (2003). Transmission dynamics and control of severe acute respiratory syndrome. *Science*, *300*(5627), 1966–1970.

Liu, R., Leung, R. K., Chen, T., Zhang, X., Chen, F., Chen, S., & Zhao, J. (2015). The Effectiveness of Age-Specific Isolation Policies on Epidemics of Influenza A (H1N1) in a Large City in Central South China. *PLOS ONE*, *10*(7), e0132588. https://doi.org/10.1371/journal.pone.0132588.

Longini, I. M., Halloran, M. E., Nizam, A., & Yang, Y. (2004). Containing Pandemic Influenza with Antiviral Agents. *American Journal of Epidemiology*, *159*(7), 623–633. https://doi.org/10.1093/aje/kwh092.

Longini, I. M., Nizam, A., Xu, S., Ungchusak, K., Hanshaoworakul, W., Cummings, D. A. T., & Halloran, M. E. (2005). Containing Pandemic Influenza at the Source. *Science*, *309*(5737), 1083–1087. https://doi.org/10.1126/science.1115717.

Luo, G., Zhang, X., Zheng, H., & He, D. (2021). Infection fatality ratio and case fatality ratio of COVID-19. *International Journal of Infectious Diseases*, *113*, 43–46.

Madhav, N., Oppenheim, B., Gallivan, M., Mulembakani, P., Rubin, E., & Wolfe, N. (2017). Pandemics: Risks, Impacts, and Mitigation. In D. T. Jamison, H. Gelband, S. Horton, P. Jha, R. Laxminarayan, C. N. Mock, & R. Nugent (Eds.), *Disease Control Priorities: Improving Health and Reducing Poverty* (3rd ed.). The International Bank for Reconstruction and Development/ The World Bank. http://www.ncbi.nlm.nih.gov/books/NBK525302/.

Madhav, N., Stephenson, N., & Oppenheim, B. (2021). *Multipathogen event catalogs—Technical note.* 24.

Majumder, M. S., Rivers, C., Lofgren, E., & Fisman, D. (2014). Estimation of MERS-coronavirus reproductive number and case fatality rate for the spring 2014 Saudi Arabia outbreak: Insights from publicly available data. *PLoS Currents Outbreaks*, *1*, doi: 10.1371/currents. outbreaks.98d2f8f3382d84f390736cd5f5fe133c.

Martinez, D. L., & Das, T. K. (2014). Design of non-pharmaceutical intervention strategies for pandemic influenza outbreaks. *BMC Public Health*, *14*(1), 1–14.

McAloon, C., Collins, Á., Hunt, K., Barber, A., Byrne, A. W., Butler, F., Casey, M., Griffin, J., Lane, E., McEvoy, D., Wall, P., Green, M., O'Grady, L., & More, S. J. (2020). Incubation period of COVID-19: A rapid systematic review and meta-analysis of observational research. *BMJ Open*, *10*(8), e039652. https://doi.org/10.1136/bmjopen-2020-039652.

Meadows, A. J., Oppenheim, B., Guerrero, J., Ash, B., Badker, R., Lam, C. K., Pardee, C., Ngoon, C., Savage, P. T., & Sridharan, V. (2022). Infectious Disease Underreporting Is Predicted by Country-Level Preparedness, Politics, and Pathogen Severity. *Health Security*, *20*(4), 331–338.

Merler, S., Ajelli, M., Pugliese, A., & Ferguson, N. M. (2011). Determinants of the Spatiotemporal Dynamics of the 2009 H1N1 Pandemic in Europe: Implications for Real-Time Modelling. *PLOS Computational Biology*, 7(9), e1002205. https://doi.org/10.1371/journal.pcbi.1002205.

Messina, J. P., Kraemer, M. U., Brady, O. J., Pigott, D. M., Shearer, F. M., Weiss, D. J., Golding, N., Ruktanonchai, C. W., Gething, P. W., Cohn, E., Brownstein, J. S., Khan, K., Tatem, A. J., Jaenisch, T., Murray, C. J., Marinho, F., Scott, T. W., & Hay, S. I. (2016). Mapping global environmental suitability for Zika virus. *ELife*, *5*, e15272. https://doi.org/10.7554/eLife.15272.

Mihigo, R., Torrealba, C. V., Coninx, K., Nshimirimana, D., Kieny, M. P., Carrasco, P., Hedman, L., & Widdowson, M.-A. (2012). 2009 Pandemic Influenza A Virus Subtype H1N1 Vaccination in Africa—Successes and Challenges. *The Journal of Infectious Diseases*, *206*(suppl_1), S22–S28. https://doi.org/10.1093/infdis/jis535.

Morens, D. M., Taubenberger, J. K., Folkers, G. K., & Fauci, A. S. (2010). Pandemic influenza's 500th anniversary. *Clinical Infectious Diseases*, *51*(12), 1442–1444.

Nichol, K. L., & Treanor, J. J. (2006). Vaccines for seasonal and pandemic influenza. *The Journal of Infectious Diseases*, *194*(Supplement_2), S111–S118.

OAG. (2016). *Reference data*. www.oag.com.

Oliveira, W. K. de, Carmo*, E. H., Penna, G. O., Kuchenbecker, R. de S., Santos, H. B., Araújo, W. N. de, Malaguti, R., Duncan, B. B., Schmidt, M. I., & Surveillance Team for the pandemic influenza A(H1N1) 2009 in the Ministry of Health. (2009). Pandemic H1N1 influenza in Brazil: Analysis of the first 34,506 notified cases of influenza-like illness with severe acute respiratory infection (SARI). *Eurosurveillance*, *14*(42).

Oppenheim, B., Gallivan, M., Madhav, N. K., Brown, N., Serhiyenko, V., Wolfe, N. D., & Ayscue, P. (2019). Assessing global preparedness for the next pandemic: Development and application of an Epidemic Preparedness Index. *BMJ Global Health*, *4*(1). https://doi.org/10.1136/bmjgh-2018-001157.

Oppenheim, B., Stephenson, N., Madhav, N. K., Jamison, D. T., Alawan, A., Brown, K., Chowell, G., Dodson, K., Euren, J., Guerrero, J., Kreuder-Johnson, C., Lam, C., Waldman, R., Yamey, G., & Steven, D. (n.d.). *The Value is in the Network: The Impact of Multilateral Cooperation on the COVID-19 Pandemic [working paper]* [(In prep)].

Presanis, A. M., Angelis, D. D., Hagy, A., Reed, C., Riley, S., Cooper, B. S., Finelli, L., Biedrzycki, P., & Lipsitch, M. (2009). The Severity of Pandemic H1N1 Influenza in the United States, from April to July 2009: A Bayesian Analysis. *PLOS Medicine*, *6*(12), e1000207. https://doi.org/10.1371/journal.pmed.1000207.

Rambaut, Andrew. (n.d.). *MERS Cases*. Retrieved April 3, 2017, from https://github.com/rambaut/MERS-Cases.

Richie, H., Mathieu, E., Rodés-Guirao, L., Appel, C., Giattino, C., Ortiz-Ospina, E., Hasell, J., Macdonald, B., Beltekian, D., & Roser, M. (2021). *Coronavirus Pandemic (COVID-19) Vaccination Data*. Published Online at OurWorldInData.Org. 'https://ourworldindata.org/coronavirus' [Online Resource].

Rivers, C. M., Majumder, M. S., & Lofgren, E. T. (2016). Risks of Death and Severe Disease in Patients With Middle East Respiratory Syndrome Coronavirus, 2012–2015. *American Journal of Epidemiology*, *184*(6), 460–464. https://doi.org/10.1093/aje/kww013.

Rizzo, C., Ajelli, M., Merler, S., Pugliese, A., Barbetta, I., Salmaso, S., & Manfredi, P. (2011). Epidemiology and transmission dynamics of the 1918–19 pandemic influenza in Florence, Italy. *Vaccine*, *29*, B27–B32. https://doi.org/10.1016/j.vaccine.2011.02.049.

Rvachev, L. A., & Longini, I. M. (1985). A mathematical model for the global spread of influenza. *Mathematical Biosciences*, *75*(1), 3–22. https://doi.org/10.1016/0025-5564(85)90064-1.

Shrestha, S. S., Swerdlow, D. L., Borse, R. H., Prabhu, V. S., Finelli, L., Atkins, C. Y., Owusu-Edusei, K., Bell, B., Mead, P. S., Biggerstaff, M., Brammer, L., Davidson, H., Jernigan, D., Jhung, M. A., Kamimoto, L. A., Merlin, T. L., Nowell, M., Redd, S. C., Reed, C., … & Meltzer, M. I. (2011). Estimating the Burden of 2009 Pandemic Influenza A (H1N1) in the United States (April 2009–April 2010). *Clinical Infectious Diseases*, *52*(suppl_1), S75–S82. https://doi.org/10.1093/cid/ciq012.

Shubin, M., Virtanen, M., Toikkanen, S., Lyytikäinen, O., & Auranen, K. (2014). Estimating the burden of A(H1N1)pdm09 influenza in Finland during two seasons. *Epidemiology & Infection*, *142*(5), 964–974. https://doi.org/10.1017/S0950268813002537.

Sikkema, R. S., Farag, E. A. B. A., Islam, M., Atta, M., Reusken, C. B. E. M., Al-Hajri, M. M., & Koopmans, M. P. G. (2019). Global status of Middle East respiratory syndrome coronavirus in dromedary camels: A systematic review. *Epidemiology and Infection*, *147*, e84. https://doi.org/10.1017/S095026881800345X.

Tai, W., Zhang, X., Yang, Y., Zhu, J., & Du, L. (2022). Advances in mRNA and other vaccines against MERS-CoV. *Translational Research*, *242*, 20–37.

Tizzoni, M., Bajardi, P., Poletto, C., Ramasco, J. J., Balcan, D., Gonçalves, B., Perra, N., Colizza, V., & Vespignani, A. (2012). Real-time numerical forecast of global epidemic spreading: Case study of 2009 A/H1N1pdm. *BMC Medicine*, *10*(1), 165.

Tuite, A. R., Greer, A. L., Whelan, M., Winter, A.-L., Lee, B., Yan, P., Wu, J., Moghadas, S., Buckeridge, D., Pourbohloul, B., & Fisman, D. N. (2010). Estimated epidemiologic parameters and morbidity associated with pandemic H1N1 influenza. *Canadian Medical Association Journal*, *182*(2), 131–136. https://doi.org/10.1503/cmaj.091807.

United Nations. (2015). *World Population Prospects: The 2015 Revision, Key Findings and Advance Tables*. United Nations.

United Nations. (2021). *Our Common Agenda—Report of the Secretary-General*.

United Nations, Department of Economic and Social Affairs, Population Division. (2022). *World Population Prospects 2022: Data Sources. (UN DESA/POP/2022/DC/NO. 9)*. https://population.un.org/wpp/.

Valleron, A.-J., Cori, A., Valtat, S., Meurisse, S., Carrat, F., & Boëlle, P.-Y. (2010). Transmissibility and geographic spread of the 1889 influenza pandemic. *Proceedings of the National Academy of Sciences*, *107*(19), 8778–8781. https://doi.org/10.1073/pnas.1000886107.

White, L. F., & Pagano, M. (2008). Transmissibility of the influenza virus in the 1918 pandemic. *PLoS One*, *3*(1), e1498.

White, L. F., Wallinga Jacco, Finelli, L., Reed, C., Riley, S., Lipsitch, M., & Pagano Marcello. (2009). Estimation of the reproductive number and the serial interval in early phase of the 2009 influenza A/H1N1 pandemic in the USA. *Influenza and Other Respiratory Viruses*, *3*(6), 267–276. https://doi.org/10.1111/j.1750-2659.2009.00106.x.

Wong, J. Y., Kelly, H., Ip, D. K. M., Wu, J. T., Leung, G. M., & Cowling, B. J. (2013). Case fatality risk of influenza A (H1N1pdm09): A systematic review. *Epidemiology (Cambridge, Mass.)*, *24*(6). https://doi.org/10.1097/EDE.0b013e3182a67448.

World Health Organization. (2009). Transmission dynamics and impact of pandemic influenza A (H1N1) 2009 virus. *Weekly Epidemiological Record = Relevé Épidémiologique Hebdomadaire*, *84*(46), 481–484.

World Health Organization. (2013). *Global survey on National Vaccine Deployment and Vaccination Plans for pandemic A (H1N1) 2009 vaccine—2010*. World Health Organization.

World Health Organization. (2015). *Summary of probable SARS cases with onset of illness from 1 November 2002 to 31 July 2003*. http://www.who.int/csr/sars/country/table2004_04_21/en/.

Wu, J. T., Ma, E. S. K., Lee, C. K., Chu, D. K. W., Ho, P.-L., Shen, A. L., Ho, A., Hung, I. F. N., Riley, S., Ho, L. M., Lin, C. K., Tsang, T., Lo, S.-V., Lau, Y.-L., Leung, G. M., Cowling, B. J., & Peiris, J. S. M. (2010). The Infection Attack Rate and Severity of 2009 Pandemic H1N1 Influenza in Hong Kong. *Clinical Infectious Diseases*, *51*(10), 1184–1191. https://doi.org/10.1086/656740.

Wu, J. T., Riley, S., Fraser, C., & Leung, G. M. (2006). Reducing the impact of the next influenza pandemic using household-based public health interventions. *PLoS Medicine*, *3*(9), e361.

Yang, Y., Sugimoto, J. D., Halloran, M. E., Basta, N. E., Chao, D. L., Matrajt, L., Potter, G., Kenah, E., & Longini, I. M. (2009). The Transmissibility and Control of Pandemic Influenza A (H1N1) Virus. *Science (New York, N.Y.)*, *326*(5953), 729–733. https://doi.org/10.1126/science.1177373.

Zhang Shenghai, Yan, P., Winchester Brian, & Wang Jun. (2009). Transmissibility of the 1918 pandemic influenza in Montreal and Winnipeg of Canada. *Influenza and Other Respiratory Viruses*, *4*(1), 27–31. https://doi.org/10.1111/j.1750-2659.2009.00117.x.

Annex B. Country regional groupings

TABLE B1. Country regional groupings

Central and Eastern Europe	Central Asia	China	India	Latin America and Caribbean	Middle East and North Africa	North Atlantic	Sub-Saharan Africa	Western Pacific and Asia
Albania	Afghanistan			Argentina	Algeria	Austria	Angola	Australia
Armenia	Azerbaijan			Bahamas, The	Bahrain	Belgium	Benin	Bangladesh
Belarus	Kazakhstan			Barbados	Egypt, Arab Rep.	Canada	Botswana	Bhutan
Bosnia and Herzegovina	Kyrgyz Republic			Belize	Iran, Islamic Rep.	Cyprus	Burkina Faso	Brunei Darussalam
Bulgaria	Mongolia			Bolivia	Iraq	Denmark	Burundi	Cambodia
Croatia	Pakistan			Brazil	Israel	Finland	Cabo Verde	Fiji
Czech Republic	Tajikistan			Chile	Jordan	France	Cameroon	Indonesia
Estonia	Turkmenistan			Colombia	Kuwait	Germany	Central African Republic	Japan
Georgia	Uzbekistan			Costa Rica	Lebanon	Greece	Chad	Korea, Dem. People's Rep.
Hungary				Cuba	Libya	Iceland	Comoros	Korea, Rep.
Latvia				Dominica	Morocco	Ireland	Congo, Dem. Rep.	Lao PDR
Lithuania				Dominican Republic	Oman	Italy	Congo, Rep.	Malaysia
Moldova				Ecuador	Qatar	Luxembourg	Cote d'Ivoire	Maldives
Montenegro				El Salvador	Saudi Arabia	Malta	Djibouti	Myanmar
North Macedonia				Guatemala	Syrian Arab Republic	Netherlands	Equatorial Guinea	NA
Poland				Guyana	Tunisia	Norway	Eritrea	Nepal
Romania				Haiti	Turkey	Portugal	Eswatini	New Zealand
Russian Federation				Honduras	United Arab Emirates	Spain	Ethiopia	Papua New Guinea
Serbia				Jamaica	West Bank and Gaza	Sweden	Gabon	Philippines
Slovak Republic				Mexico	Yemen, Rep.	Switzerland	Gambia, The	Singapore
Slovenia				Nicaragua		United Kingdom	Ghana	Solomon Islands

Central and Eastern Europe	Central Asia	China	India	Latin America and Caribbean	Middle East and North Africa	North Atlantic	Sub-Saharan Africa	Western Pacific and Asia
Ukraine				Panama		United States	Guinea	Sri Lanka
				Paraguay			Guinea–Bissau	Thailand
				Peru			Kenya	Timor-Leste
				Puerto Rico			Lesotho	Tonga
				Suriname			Liberia	Vanuatu
				Trinidad and Tobago			Madagascar	Vietnam
				Uruguay			Malawi	
				Venezuela, RB			Mali	
							Mauritania	
							Mauritius	
							Mozambique	
							Namibia	
							Niger	
							Nigeria	
							Rwanda	
							Senegal	
							Seychelles	
							Sierra Leone	
							Somalia	
							South Africa	
							South Sudan	
							Sudan	
							Tanzania	
							Togo	
							Uganda	
							Zambia	
							Zimbabwe	

Note: This grouping may be subject to change in future revisions of this paper.